PHYSICAL REVIEW B **84**, 205136 (2011)

Bulk-edge correspondence in entanglement spectra

Anushya Chandran,[1] M. Hermanns,[1] N. Regnault,[2] and B. Andrei Bernevig[1]
[1]*Department of Physics, Princeton University, Princeton, New Jersey 08544, USA*
[2]*Laboratoire Pierre Aigrain, ENS and CNRS, 24 rue Lhomond, FR-75005 Paris, France*
(Received 22 February 2011; revised manuscript received 25 October 2011; published 22 November 2011)

Li and Haldane conjectured and numerically substantiated that the entanglement spectrum of the reduced density matrix of *ground states* of time-reversal-breaking topological phases [fractional quantum Hall (FQH) states] contains information about the counting of their edge modes when the ground state is cut in two spatially distinct regions and one of the regions is traced out. We analytically substantiate this conjecture for a series of FQH states defined as unique zero modes of pseudopotential Hamiltonians by finding a one-to-one map between the thermodynamic limit counting of two different entanglement spectra: the particle entanglement spectrum (PES), whose counting of eigenvalues for each good quantum number is identical to the counting of bulk quasiholes (up to accidental zero eigenvalues of the reduced density matrix), and the orbital entanglement spectrum (OES), considered by Li and Haldane. By using a set of clustering operators that have their origin in conformal-field-theory (CFT) operator expansions, we show that the counting of the OES eigenvalues in the thermodynamic limit must be identical to the counting of quasiholes *in the bulk*. The latter equals the counting of edge modes at a hard-wall boundary placed on the sample. Our results can be interpreted as a bulk-edge correspondence *in entanglement spectra*. Moreover, we show that the counting of the PES and OES is identical even for CFT states that are likely bulk gapless, such as the Gaffnian wave function.

DOI: 10.1103/PhysRevB.84.205136 PACS number(s): 63.22.−m, 87.10.−e, 63.20.Pw

I. INTRODUCTION

Determining the universality class of a real system exhibiting a topological phase is a difficult task in condensed matter physics. Renormalization-group methods have been very successful in uncovering the universal physics in phases with local order parameters, but, due to their perturbative approach, can not be readily generalized to topological phases that do not exhibit symmetry breaking. The density-matrix renormalization group[1–4] and tensor-matrix product states[5,6] can probe topological order in one dimension, but have had limited success with higher-dimensional systems so far. The prototype of two-dimensional topologically ordered phases are the experimentally accessible fractional quantum Hall (FQH) phases. A promising tool to extract topological information from the ground-state wave function in these phases is the entanglement entropy.[7–11] However, it depends on scaling arguments, is hard to obtain to sufficient accuracy from numerical calculations,[12,13] and does not uniquely determine the topological order in the state.

In 2008, Li and Haldane[14] proposed a new tool to identify topological order in non-Abelian FQH states—the entanglement spectrum. They divided the single-particle orbitals in a Landau level on the sphere along the equator and constructed the reduced density matrix of the ideal (model) and the realistic (Coulomb) FQH states in the upper half of the sphere (part A) by tracing out orbitals in the lower half (part B). Having thus created a "virtual" edge, they defined the orbital entanglement spectrum (OES) to be the plot of the negative logarithm of the eigenvalues of the reduced density matrix of A versus the z angular momentum of A (L_z^A) for a fixed number of particles in A. In particular, Li and Haldane considered the part of the spectrum with the lowest-lying levels and the highest-weight eigenstates of the reduced density matrix of A. They noticed that the number of levels in every OES of the model states, such as the Laughlin and the Moore-Read, was much smaller than the Hilbert space dimension and was identical to the counting of the conformal-field-theory (CFT) modes associated with the edge at large values of L_z^A. Although the number of levels in the OES of the Coulomb state saturated the Hilbert space dimension, a gap separated the levels higher in the spectrum from a CFT-like low-lying spectrum at small values of L_z^A with the *same* counting as the model state. This was taken as evidence that the Coulomb state at $\nu = 5/2$ and the model Pfaffian state belonged to the same universality class. Based on extensive numerical evidence, they conjectured the following: (1) In the thermodynamic limit, the counting of the OES (i.e., the number of nonzero eigenvalues of the reduced density matrix) of the model state is the counting of the modes of the conformal theory describing its gapless edge excitations. (2) The "entanglement gap" separating the low-lying, CFT-like levels from the generic ones higher in the Coulomb spectrum is finite in the thermodynamic limit.

Many researchers have investigated properties of the entanglement spectra since. The authors of Ref. 15 discovered that the entanglement spectrum in the thin-annulus limit (the conformal limit) had, for several examples, a *full* gap at finite system sizes. The counting of the *entire* low-lying spectrum of the Coulomb state is the same as that of the corresponding model state in this limit. Motivated by this result, we recently conjectured a counting principle for the finite-size counting of the OES of the Laughlin states.[16] Other cuts have also been studied. Tracing out a fraction of the particles in the many-body ground state corresponds to a particle cut; the entanglement spectrum of the resulting reduced density matrix is the particle entanglement spectrum (PES) introduced in Ref. 17. The level counting of the PES of a model state (described as a CFT correlator) is bounded from above by the number of *bulk* quasihole states of the model state; along with the OES, it is conjectured to contain all the topological numbers of the state. Entanglement spectra in other systems have also been explored; see, for instance, Refs. 18–35.

Analytic work in this emerging field is challenging because of the strongly interacting nature of FQH states. The Li-Haldane conjecture (the correspondence between the counting of the number of modes of the real-space spectrum in the thermodynamic limit and the counting of the edge-excitation spectrum) is easy to prove in noninteracting systems, such as the integer quantum Hall system and topological insulators.[36–38]

In this paper, we partially prove the first part of the Li-Haldane conjecture for clustering model states: in the thermodynamic limit, we show that the counting of the CFT associated with the edge is an upper bound of the counting of the low-lying levels of the OES. We give physical arguments for why this bound should be saturated. We prove the upper bound for the bosonic $(k,2)$-clustering states (the Read-Rezayi sequence) multiplied by any number of Jastrow factors, and for the Gaffnian. In principle, this should hold for all model states defined as the unique, highest-density zero modes of $(k+1)$-body pseudopotential Hamiltonians.[39] This proof is obtained by establishing a bulk-edge correspondence in the entanglement spectra: the particle and orbital entanglement spectra have the same counting for the range of parameters that become the most relevant in the thermodynamic limit. For finite-size systems, the correspondence holds for the counting at large angular momenta.

The paper is organized as follows: Our notation is introduced in Sec. II. We define the orbital entanglement matrix and spectrum in Sec. III and the particle entanglement matrix and spectrum in Sec. IV. In Sec. IV C, we present the upper bound to the number of levels in the particle entanglement spectrum and argue for its saturation. In Sec. V, we formulate the clustering properties of the model state in the single-particle orbital basis. We use them to relate the counting of the particle and orbital entanglement spectra of the Read-Rezayi sequence in Sec. VI. The parameter range for which the bulk-edge correspondence holds is presented in Sec. VI B. The proof for the upper bound of the Li-Haldane conjecture is presented at the end of the same section. In Sec. VI D, we extend the proof to the other model states. Examples and the mathematical formulation of the ideas in the proof are in the Appendices.

II. NOTATION

The results that we present in this paper hold on any surface of genus 0 (such as the disk or the sphere) pierced by N_ϕ flux quanta; for simplicity, we choose the sphere geometry. The single-particle states of each Landau level are eigenstates of $\hat{L}_z$, the z component of angular momentum and $|\vec{L}|^2$, the square of the magnitude of the total angular momentum vector.[40] In the lowest Landau level, the degenerate single-particle states belong to a multiplet of angular momentum $L = N_\phi/2$ and, consequently, $L_z \in [-N_\phi/2, \ldots, N_\phi/2]$. Identifying the coordinate $z = \tan\theta e^{i\phi}$, where θ and ϕ are the two angles that parametrize the sphere, the unnormalized monomials

$$\langle z|m\rangle = z^m, \quad m = \frac{N_\phi}{2} - L_z \tag{1}$$

span the lowest Landau level and will be our single-particle basis of choice in this paper. We are forced to adopt a dual notation in this paper: the single-particle orbitals are indexed by their z angular momentum L_z in the figures and by a shifted label $m = (N_\phi/2 - L_z)$ in the text. At the north (south) pole, $L_z = N_\phi/2$ $(-N_\phi/2)$.

Fermionic and bosonic many-body wave functions of N particles and total angular momentum L_z^{tot} can be expressed as linear combinations of Fock states in the occupation-number basis of the single-particle orbitals. Each Fock state $|\lambda\rangle$ can be labeled either by the list of occupied orbitals λ or by the occupation-number configuration $n(\lambda)$. $\lambda = [\lambda_1, \lambda_2, \ldots, \lambda_N]$ is an ordered partition of L_z^{tot} into N parts and each orbital with index λ_j is occupied in the Fock state. By definition, $\lambda_i \geqslant \lambda_j$ if $i < j$. $n(\lambda)$ is the occupation-number configuration. It is defined as $n(\lambda) = \{n_j(\lambda), j = 0, \ldots N_\phi\}$, where $n_j(\lambda)$ is the occupation number of the single-particle orbital with angular momentum j. In the unnormalized polynomial basis,

$$\langle z_1, \ldots, z_N|\lambda\rangle = S\left[z_1^{\lambda_1} \cdot \ldots \cdot z_N^{\lambda_N}\right], \tag{2}$$

where S is the process of symmetrization and antisymmetrization over all indices i, j such that $\lambda_i \neq \lambda_j$. For example, if $N_\phi = 2$ and $N = 2$, orbitals 2 and 0 are occupied in the Fock state $|2,0\rangle$ of the three available orbitals. Consequently, $\lambda = [2,0]$, $n(\lambda) = \{101\}$, and $\langle z_1, z_2|2,0\rangle = z_1^2 + z_2^2$. Similarly, $\lambda = [1,1]$, $n(\lambda) = \{020\}$, and $\langle z_1, z_2|1,1\rangle = z_1 z_2$ for the other Fock state at the same total angular momentum.

We will repeatedly run into a special kind of partition in this paper, i.e., the (k,r)-admissible partition. A (k,r)-admissible partition labels a Fock state, the occupation configuration of which has no more than k particles in r consecutive orbitals. These partitions play a prominent role in our discussions as they count the Hilbert space of the quasiholes of our model FQH liquids, which have generalized (k,r)-exclusion Haldane statistics.[41] For the examples above, $\lambda = [2,0]$ is $(1,2)$ admissible, while $[1,1]$ is not.

Three useful relations between partitions are "dominance," "squeezing," and "addition." A set of partitions may always be partially ordered by dominance, indicated by the symbol $>$. A partition μ dominates another partition ν $(\mu > \nu)$ if $\sum_{i=0}^{r} \mu_i \geqslant \sum_{i=0}^{r} \nu_i \; \forall r \in [0, \ldots, N]$. Squeezing is a two-particle operation that connects $n(\mu)$ to $n(\nu)$. It modifies the orbitals occupied by any two particles in $n(\mu)$ from m_1 and m_2 to m_1' and m_2' in $n(\nu)$, such that $m_1 + m_2 = m_1' + m_2'$ and $m_1 < m_1' \leqslant m_2' < m_2$ if the particles are bosonic or $m_1 < m_1' < m_2' < m_2$ if they are fermionic. Dominance and squeezing are identical concepts: a partition μ dominates a partition ν if ν can be squeezed from μ by a series of squeezing operations. The "sum" of two partitions $\mu + \nu$ is defined as the partition with occupation configuration $n(\mu + \nu) = \{n_j(\mu) + n_j(\nu), j = 0, \ldots N_\phi\}$.

FQH wave functions in the lowest Landau level are translationally invariant, symmetric, homogeneous polynomials of the coordinates of the N particles $(z_1, z_2, \ldots, z_N)$. We consider mainly the bosonic Read-Rezayi sequence at filling $\nu = k/2$ here (see Sec. VI D for other model states). These states are the unique, highest-density zero-mode wave functions of $(k+1)$-body pseudopotential Hamiltonians.[39] Recent work[42] has shown the Read-Rezayi bosonic wave functions ψ to be Jack polynomials $J_{\lambda_0}^{\alpha}$ indexed by a parameter $\alpha = -(k+1)$ and the densest possible $(k,2)$-admissible root configuration[43]

$$n(\lambda_0) = \{k0k0k0 \ldots k0k\}. \tag{3}$$

For the $(k,2)$-clustering states, the number of fluxes for the ground-state wave function is $N_\phi = 2(N/k - 1)$. All the Jack polynomials at $\alpha = -(k+1)$ indexed by $(k,2)$-admissible root configurations are $(k,2)$-clustering polynomials, i.e., they vanish as $\prod_{i>k}(z - z_i)^2$ when $z = z_1 = \ldots z_k$. They form a basis for all many-body $(k,2)$-clustering polynomials and can be decomposed into a linear combination of Fock states with configurations squeezed from the root partition. Importantly for us, they span the *entire* zero-mode space of the $(k+1)$-body hard-core model Hamiltonian consisting of the ground state and all the quasihole states.[42] They provide a natural description of the particle entanglement spectrum as we shall see in Sec. IV C.

III. ORBITAL ENTANGLEMENT MATRIX

A. Definition

Consider dividing the set of single-particle orbitals $\{0,1,\ldots,N_\phi\}$ into two disjoint sets $A = \{0,1,\ldots,l_A - 1\}$ and $B = \{l_A,\ldots,N_\phi\}$. As the single-particle orbitals are polynomially localized in the $\hat{\theta}$ direction, this partition in the single-particle momentum space roughly corresponds to an azimuthally symmetric spatial cut.

The number of orbitals in A (B) is l_A (l_B), where $l_B = N_\phi + 1 - l_A$. Without loss of generality, let $l_A \leqslant l_B$ $(l_A \geqslant l_B$ for A and B swapped). Any occupation number state $|\lambda\rangle$ may be expressed as a tensor product $|\mu\rangle \otimes |\nu\rangle$ of states with partitions μ and ν belonging to the Hilbert spaces of A and B, respectively. Thus, the model state can be decomposed as

$$|\psi\rangle = \sum_\lambda b_\lambda |\lambda\rangle = \sum_{i,j} (\mathbf{C_f})_{ij} |\mu_i\rangle \otimes |\nu_j\rangle, \tag{4}$$

where the kets $\{|\mu_i\rangle\}$ and $\{|\nu_j\rangle\}$ form orthonormal bases that span the Hilbert spaces of A and B. Note that, for an orbital cut, all terms in the decomposition are totally symmetric in all the particles. This is not the case for the particle cut that is discussed in Sec. IV. The matrix $\mathbf{C_f}$ is the full orbital entanglement matrix (OEM). The (i,j)th matrix element of the full OEM is equal to the coefficient of $|\mu_i + \nu_j\rangle$ in $|\psi\rangle$:

$$(\mathbf{C_f})_{ij} = b_{\mu_i + \nu_j}\,. \tag{5}$$

In this paper, we will almost exclusively deal with entanglement matrices. Unless stated otherwise, the rows (columns) of these matrices, for both the OEM defined in Eq. (4) and for the PEM defined below, will be labeled by partitions μ_i (ν_j) corresponding to the occupation basis states $|\mu_i\rangle$ $(|\nu_j\rangle)$ in A (B). The vector defined by the entries of a row and column in the entanglement matrix shall be referred to as row/column vector.

Readers unfamiliar with the OEM and how to construct it are encouraged to take a look at Appendix A, where we explicitly construct the OEM for a simple example.

B. Properties

$\mathbf{C_f}$ has a block-diagonal form; each block in the full OEM $\mathbf{C}_f$ is labeled by N_A, the number of particles in A, and L_z^A, the total z angular momentum of the N_A particles in A. Note that $L_z^A = \sum_{i=1}^{N_A} \mu_i$ for the state $|\mu\rangle$, where μ_i here are the components of the partition μ. Due to an unfortunate but necessary choice of notation, μ_i also index the partitions of the Hilbert space of part A. In that case, μ_i is a partition by itself, and its components are $\mu_{i1},\mu_{i2},\ldots,\mu_{iN_A}$. The use of μ_i as a partition or as a component of a partition μ will be self-evident in the text. To understand the origin of the block-diagonal structure of $\mathbf{C_f}$, observe that $|\psi\rangle$ is an eigenstate of the particle-number operator $\hat{N}$ and the total z angular momentum operator $\hat{L_z^{\rm tot}}$. As both operators are sums of one-body operators, $\hat{N} = \hat{N}_A \otimes \mathbb{I} + \mathbb{I} \otimes \hat{N}_B$ and $\hat{L_z^{\rm tot}} = \hat{L_z^A} \otimes \mathbb{I} + \mathbb{I} \otimes \hat{L_z^B}$. Thus, every $|\lambda\rangle$ in Eq. (4) is labeled by the quantum numbers N and $L_z^{\rm tot}$, while every $|\mu_i\rangle$ $(|\nu_j\rangle)$ is labeled by N_A $(N_B = N - N_A)$ and L_z^A $(L_z^B = L_z^{\rm tot} - L_z^A)$. In the remainder of this paper, the symbol $\mathbf{C}$ refers to the block of the full OEM $\mathbf{C_f}$ with labels N_A and L_z^A.

The reduced density matrices are obtained from $\mathbf{C_f}$ as $\boldsymbol{\rho}_A = \mathbf{C_f}\mathbf{C_f}^\dagger$ and $\boldsymbol{\rho}_B = \mathbf{C_f}^\dagger\mathbf{C_f}$. The block-diagonal structure of $\mathbf{C_f}$ carries over to the reduced density matrices and the rank of $\boldsymbol{\rho}_A$ and $\boldsymbol{\rho}_B$ in each block is equal to that of $\mathbf{C}$. Neither $\boldsymbol{\rho}_A$ nor $\boldsymbol{\rho}_B$ uniquely determine all the coefficients of $|\psi\rangle$; $\mathbf{C_f}$ clearly contains more information than either of the reduced density matrices.

The singular value decomposition of $\mathbf{C}$ is given by

$$\sum_{i,j} \mathbf{C}_{ij} |\mu_i\rangle \otimes |\nu_j\rangle = \sum_{i=1}^{\mathrm{rank}(\mathbf{C})} e^{-\xi_i/2} |U_i\rangle \otimes |V_i\rangle. \tag{6}$$

The kets on the left-hand side of Eq. (6) are defined as in Eq. (4). $|U_i\rangle$ and $|V_i\rangle$ are the singular vectors in the Hilbert spaces of A and B restricted to a fixed particle number and z angular momentum. They are linear combinations of the occupation-number basis vectors $|\mu_i\rangle$ and $|\nu_j\rangle$. The ξ_i's are the energies plotted as a function of L_z^A in the orbital entanglement spectrum (OES) introduced in Ref. 14.

The number of finite energies [rank$(\mathbf{C})$] at each (N_A, L_z^A) is independent of the geometry of the two-dimensional (2D) surface and the symmetrization factors arising due to multiple particles occupying the same orbital. Let $\mathbf{C_f}^d$ and $\mathbf{C_f}^s$ be the full OEMs in the disk and sphere geometry, or in any other two genus 0 geometries. Modifying the geometry of the surface changes the normalization of the single-particle orbitals (the quantum mechanical normalization); thus, every b_λ in the expansion of $|\psi\rangle$ in Eq. (4) in the disk basis is multiplied by a factor $\mathcal{N}(\lambda) = \prod_{i=1}^N \mathcal{N}(\lambda_i)$ when expanded in the single-particle orbital basis on the sphere. $\mathcal{N}(j)$ is a factor relating the normalization of orbital j on the disk to that on the sphere. The OEMs on the disk and the sphere are thus related as

$$\begin{aligned} |\psi\rangle &= \sum_{i,j} \left(\mathbf{C_f}^d\right)_{ij} \left|\mu_i^d\right\rangle \otimes \left|\nu_j^d\right\rangle \\ &= \sum_{i,j} \left(\mathbf{C_f}^d\right)_{ij} \mathcal{N}\left(\mu_i^d\right)\mathcal{N}\left(\nu_j^d\right) \left|\mu_i^s\right\rangle \otimes \left|\nu_j^s\right\rangle, \end{aligned} \tag{7}$$

where the superscripts d and s refer to the disk and sphere geometries, or to any other two genus 0 geometries. $\mathbf{C_f}^s$ is obtained from $\mathbf{C_f}^d$ by multiplying whole rows and columns by normalization factors; thus, $\mathrm{rank}(\mathbf{C_f}^s) = \mathrm{rank}(\mathbf{C_f}^d)$. An identical argument shows the rank of $\mathbf{C_f}$ to be independent of the symmetrization factors that arise in the normalization of the

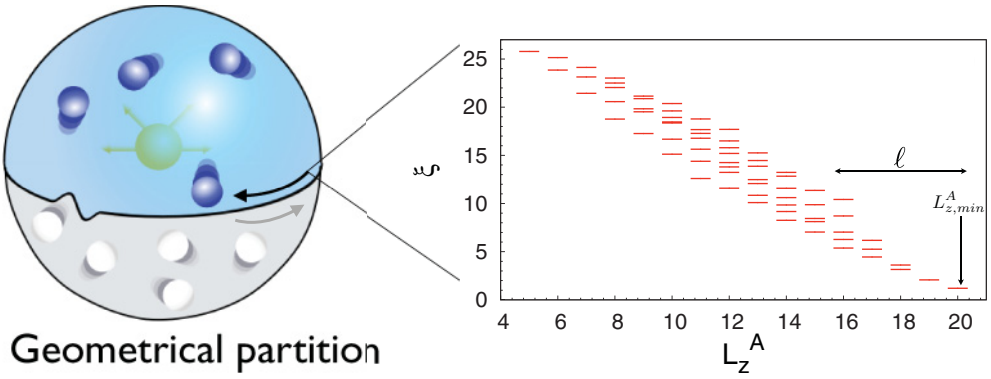

FIG. 1. (Color online) Left: Sketch of the partition in orbital space (part B in gray). The tracing procedure creates a virtual edge and the orbital entanglement spectrum (OES) probes the chiral edge mode(s) of part A. Right: OES of the $\nu = 1/2$ Laughlin state of $N = 9$ bosons, with orbital cut $l_A = 8$ and $N_A = 4$. The minimal angular momentum $L^A_{z,\min}$ defined in the text is the $L^A_{z,\min} = 20$ sector in the plot. The entanglement level counting at $\ell = |L^A_z - L^A_{z,\min}| = 0,1,\ldots,4$ is (1,1,2,3,5), which is the counting of modes of a U(1) boson in the thermodynamic limit. Finite-size effects appear at $L^A_z = 15$.

many-body states constructed from normalized single-particle orbitals. We are therefore free to work in an unnormalized single-particle basis from this point.

For a given cut l_A in orbital space, the *maximum* number of particles that can form a $(k,2)$-clustering droplet in A is defined to be the natural number of particles $N_{A,\mathrm{nat}}$:

$$N_{A,\mathrm{nat}} = k\lfloor (l_A + 1)/2 \rfloor , \tag{8}$$

where $\lfloor x \rfloor$ is the integer part of x. Physically, $N_{A,\mathrm{nat}}/l_A$ is very close to the original filling ν. We may think of the original, homogeneous QH fluid as being composed of two droplets in A and B of $N_{A,\mathrm{nat}}$ and $N_{B,\mathrm{nat}} = N - N_{A,\mathrm{nat}}$ particles each, interacting via correlated excitations along their common edge. We would thus expect the OES at $N_{A,\mathrm{nat}}$, called the natural spectrum, to be the low-energy sector of the full entanglement energy spectrum and to contain information about the edge theory of the model state. In the thermodynamic limit, the number of finite energies (level counting) of the OES is conjectured to be identical to the counting of the modes of the CFT describing the edge for values $l_A, N_A \to \infty$ such that $l_A/N_\phi \to$ const.(> 0) and $N_A/N_{A,\mathrm{nat}} \to 1$.

For future reference, $L^A_{z,\min}$ denotes the minimum z angular momentum of the N_A particles in A of a $(k,2)$-clustering model state:

$$L^A_{z,\min} = \lfloor N_A/k \rfloor (2N_A - k\lfloor N_A/k \rfloor - k). \tag{9}$$

We stress that $L^A_{z,\min}$ is the *maximum* value on the x axis of the *numerically* generated entanglement spectra existing in the literature due to the different indexing scheme in the text and the figures (see also the discussion in Sec. II). For instance, in Fig. 1, $L^A_{z,\min}$ describes the sector of the OES at $L^A_z = 20$.

For an arbitrary pure bosonic state of N particles, the rank of the OEM $\mathbf{C_f}$ must generically be the smaller of its dimensions. The model states are special because the rank of the OEM block at given (N_A, L^A_z) is in general much smaller than its smaller dimension. The rank of the OEM block at given N_A, as a function of $\ell = |L^A_z - L^A_{z,\min}|$, is called the counting of the OES (see, also, Fig. 1). For model states, it has been observed from small-size numerical calculations that the counting is universal for the first few values of ℓ,[14] i.e., independent of N, N_A, and l_A. The universal counting is distinct for each model state, which is why Li and Haldane proposed it as a way to determine the topological order[44] of the FQH states. For instance, for a Laughlin state, the universal counting is $\{1,1,2,3,5,7,11,\ldots\}$, while for the Moore-Read (MR) state, it is $\{1,1,3,5,10,16,\ldots\}$. In the OES of the Laughlin 1/2 state in Fig. 1, the counting is universal for $\ell = 0,\ldots,4$: $\{1,1,2,3,5,\ldots\}$, starting from the right edge of the spectrum. For larger ℓ, finite-size corrections occur. The universal counting is identical to counting the modes of a massless, chiral boson, which is the CFT describing the edge of the Laughlin FQH states.

IV. PARTICLE ENTANGLEMENT MATRIX

A. Definition

In the orbital cut that we just discussed, the Hilbert space of A at given (N_A, L^A_z) was spanned by the possible occupation configurations $|\mu\rangle$ of N_A particles, such that $\sum_{i=1}^{N_A} \mu_i = L^A_z$ and $\mu_i < l_A \,\forall i$. We now consider making a cut of a FQH state $|\psi\rangle$ in particle space by dividing the N particles into groups A and B with N_A and $N_B = N - N_A$ particles. Without loss of generality, let $N_A \leqslant N_B$.

Let us first consider the model state in the unnormalized real-space basis $\psi(z_1,\ldots,z_N) = \sum_\lambda b_\lambda \langle z_1,\ldots,z_N|\lambda\rangle$. For simplicity, we choose the particles at positions $\{z_1,\ldots,z_{N_A}\}$ as group A and the remaining particles $\{z_{N_A+1},\ldots,z_N\}$ as group B. Each many-body basis state $\langle z_1,\ldots,z_N|\lambda\rangle$ can be decomposed as

$$\langle z_1,\ldots,z_N|\lambda\rangle = \sum_{\mu,\nu} \langle z_1,\ldots,z_{N_A}|\mu\rangle \langle z_{N_A+1},\ldots,z_N|\nu\rangle , \tag{10}$$

where the sum runs over all partitions μ and ν of N_A and N_B particles, respectively, such that $\mu + \nu = \lambda$. In particular, there is no orbital restriction on the partitions in contrast to the orbital cut considered in the last section. Thus, the Hilbert space of A (B) is spanned by all possible occupation configurations of N_A (N_B) particles *in the full single-particle orbital basis* of the state $|\psi\rangle$. It contains the smaller Hilbert space of A (B) with

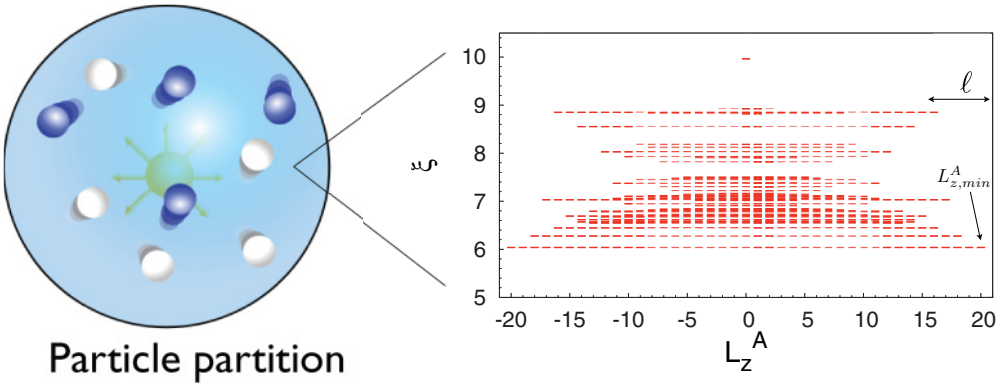

FIG. 2. (Color online) Left: Sketch of the partition in particle space. The particles of part B that are traced out are denoted in gray. Right: particle entanglement spectrum (PES) of the $\nu = 1/2$ Laughlin state of $N = 9$ bosons, with particle cut $N_A = 4$. The minimum angular momentum $L^A_{z,\min}$ defined in the text is $L^A_{z,\min} = 20$ in the plot. The entanglement level counting is identical to the counting of quasiholes in a Laughlin state of four particles with total flux $N_\phi = 16$ at all angular momenta L^A_z. For $\ell = |L^A_z - L^A_{z,\min}| = 0,1,\ldots,4$, the counting is universal, i.e., independent of N_A: (1,1,2,3,5).

the orbital restriction that only the first l_A (the last l_B) orbitals are occupied. The latter is the Hilbert space obtained from the orbital entanglement cut, but with *fixed* particle number N_A.

Just as in the preceding section, we can write the model wave function $\psi(z_1,\ldots,z_N)$ as

$$\begin{aligned}\psi(z_1,\ldots,z_N) &= \sum_\lambda b_\lambda \langle z_1,\ldots,z_N|\lambda\rangle \\ &= \sum_\lambda \sum_{\mu_i+\nu_j=\lambda} (\mathbf{P_f})_{ij} \langle z_1,\ldots,z_{N_A}|\mu_i\rangle \\ &\quad \times \langle z_{N_A+1},\ldots,z_N|\nu_j\rangle, \end{aligned} \tag{11}$$

where the summation is over all partitions μ_i (ν_j) of N_A (N_B) particles in N_ϕ orbitals. Note that each term in the second line of Eq. (11) is only symmetric in the first N_A and last $N_B = N - N_A$ particle coordinates separately; the summation ensures that the full expression is symmetric in all particle coordinates. The matrix $\mathbf{P}_f$ is the full particle entanglement matrix (PEM). As was the case for the OEM, the matrix elements of the PEM are directly related to the weights of the model wave function by

$$(\mathbf{P}_f)_{ij} = b_{\mu_i+\nu_j}. \tag{12}$$

Even though Eq. (12) looks very similar to Eq. (5), they define two different matrices because the sets of partitions $\{\mu_i\}$ and $\{\nu_i\}$, labeling the rows and columns, are different for the orbital and particle cuts. However, they are not completely unrelated as we will see in the next section.

Readers unfamiliar with the particle cut and how to construct the PEM are encouraged to look at Appendix A, where we construct the PEM explicitly for a Laughlin model state.

B. Properties

For a given cut with N_A particles in A, $\mathbf{P}_f$ is block diagonal in the angular momentum of part A, L^A_z. The block of $\mathbf{P}_f$ at fixed (L^A_z, N_A) shall be denoted by $\mathbf{P}$. The reduced density matrices of parts A and B are given by $\boldsymbol{\rho}_A = \mathbf{P}_f\mathbf{P}_f^\dagger$ and $\boldsymbol{\rho}_B = \mathbf{P}_f^\dagger\mathbf{P}_f$, respectively. They are block diagonal in L^A_z and have the same rank as $\mathbf{P}_f$ in each block. In the same spirit as the discussion of the OEM, we define the singular value decomposition of the PEM by

$$\sum_{i,j} (\mathbf{P})_{ij} |\mu_i\rangle \otimes |\nu_j\rangle = \sum_i e^{-\xi_i/2} |U_i\rangle \otimes |V_i\rangle, \tag{13}$$

where the singular vectors $|U_i\rangle$ and $|V_i\rangle$ are orthonormal vectors in the Hilbert spaces of A and B restricted to fixed angular momentum. The plot of the energies ξ_i versus L^A_z is called the particle entanglement spectrum (PES).[17] In Fig. 2, we show the PES of the 9-particle 1/2 Laughlin state for the particle cut $N_A = 4$.

In the spherical geometry, the PEM is labeled by an additional quantum number as compared to the OEM,[17] i.e., the total angular momentum of A, $(\vec{L}^A)^2$. Consequently, the eigenvalues of the block of the reduced density matrix with $(\vec{L}^A)^2 = \ell(\ell+1)$ have $(2\ell+1)$-fold degeneracy. This multiplet structure, apparent in the PES in Fig. 2, does not play any role in our discussions about the counting of the PES in this paper.

As for the OES, we can define the counting of the PES as the number of finite entanglement levels (i.e., the number of nonzero eigenvalues of the reduced density matrix) as a function of $\ell = |L^A_z - L^A_{z,\min}|$ (see, also, Fig. 2). From numerical calculations, it has been observed[17] that the counting of the PES is identical to the number of quasihole states of the model state with N_A particles in N_ϕ orbitals at all angular momenta L^A_z. For values $\ell = 0,\ldots,\lfloor N_A/k \rfloor$ we expect the counting to be universal, i.e., independent of N_A and system size. In the next section, we prove (following Ref. 17) that the counting is bounded by the number of quasihole states and argue for the saturation of the bound.

For given particle number N_A and angular momentum L^A_z, the number of entanglement levels in the OES is bounded from above by the number of entanglement levels in the PES. To see this, note that the crucial difference between Eqs. (5) and (12) is the set of partitions that label the rows and columns of the matrices. The rows (columns) of the PEM block are labeled by all partitions μ (ν) of L^A_z ($L^B_z = L^{\rm tot}_z - L^A_z$) into N_A (N_B) parts, with $0 \leqslant \mu_i \leqslant N_\phi$ ($0 \leqslant \nu_i \leqslant N_\phi$). A subset of these, namely, the ones with the restriction $0 \leqslant \mu_i \leqslant l_A - 1$

($l_A \leqslant \nu_i \leqslant N_\phi$), are the ones that label the rows (columns) of the OEM block. Thus, for fixed N_A and L_z^A the OEM block is a sub-matrix of the PEM block, which implies that its rank is smaller or equal to the rank of the PEM block, see Fig. 4. A simple, explicit example for these results can be found in Appendix A.

In Fig. 2, we show the PES of the 9-particle 1/2 Laughlin state for the particle cut $N_A = 4$. The counting is identical to the number of quasihole states of a Laughlin state with 4 particles in 16 orbitals. For $\ell = 0, \ldots, 4$, the counting of the PES is universal and identical to the counting of the OES in Fig. 1.

C. Rank

The property that defines the k-clustered model state $\psi(z_1, \ldots, z_N)$ uniquely is that it is the lowest degree symmetric polynomial that vanishes when $(k+1)$ particles are at the same position. Similar clustering conditions characterize every ground state of a pseudopotential Hamiltonian. This vanishing property must persist when we divide the particles into two groups and rewrite the model state in Eq. (11) as

$$\psi(z_1, \ldots, z_N) = \sum_{L_z^A} \sum_i e^{-\xi_i/2} \langle z_1, \ldots, z_{N_A} | U_i \rangle \langle z_{N_A+1}, \ldots, z_N | V_i \rangle, \tag{14}$$

using Eq. (13) at each L_z^A. If we choose $(k+1)$ particles in group A, say, $z_1, \ldots, z_{k+1}$, to be at the same position z, then the state must vanish at every L_z^A. Further, as the singular vectors in B form an orthonormal basis,

$$\psi(z, \ldots, z, z_{k+2}, \ldots, z_N) = 0 \Rightarrow e^{-\xi_i/2} \langle z, \ldots, z, z_{k+2}, \ldots, z_{N_A} | U_i \rangle = 0, \forall i, L_z^A . \tag{15}$$

A similar relation holds when A and B are interchanged. We conclude that the singular vectors $\langle z_1, \ldots, z_{N_A} | U_i \rangle$ and $\langle z_{N_A+1}, \ldots, z_N | V_i \rangle$ must also be clustering polynomials that vanish when $(k+1)$ particles are at the same position. A basis for clustering polynomials is the set of Jack polynomials $J_{\tilde{\mu}}^{\alpha}$, indexed by $\alpha = -(k+1)$ and the $(k,2)$-admissible partition $\tilde{\mu}$.[42,43,45] ψ can therefore be expanded in the Jack basis as

$$\psi(z_1, \ldots, z_N) = \sum_{i,j} (\mathbf{M}_f)_{ij} J_{\tilde{\mu}_i}^{\alpha}(z_1, \ldots, z_{N_A}) J_{\tilde{\nu}_j}^{\alpha}(z_{N_A+1}, \ldots, z_N), \tag{16}$$

where $\tilde{\mu}_i$ and $\tilde{\nu}_j$ denote $(k,2)$-admissible partitions of N_A and N_B particles, respectively. The matrix $\mathbf{M}_f$ is block diagonal in angular momentum L_z^A; let $\mathbf{M}$ refer to the block of $\mathbf{M_f}$ at fixed value of L_z^A. The row and column dimensions of $\mathbf{M}$ are much smaller than those of $\mathbf{P}$ because the $(k,2)$-admissible partitions of N_A and N_B form a small subset of the set of all partitions with fixed L_z^A and L_z^B, respectively. Nevertheless, as Eqs. (14) and (16) are equal, $\mathbf{M}$ and $\mathbf{P}$ must have the same rank. As $N_A \leqslant N_B$, the row dimension of $\mathbf{M}$ is smaller (or equal) than the column dimension and bounds the rank of the PEM block from above at each L_z^A.

Let us reformulate what we have just shown in a more familiar language and argue for the saturation of the bound. The row dimension of $\mathbf{M}$ is given by the number of $(k,2)$-admissible configurations of N_A particles in N_ϕ orbitals and, thus, is equal to the number of distinct bulk quasihole excitations of the $(k,2)$-clustering model state of N_A particles at angular momentum L_z^A on a sphere pierced by the number of fluxes of the original state $N_\phi = 2/k(N-k)$.[46,47] Hence, we find that the rank of the PEM is bounded by the number of quasihole states for all angular momenta L_z^A. Without further symmetry-induced constraints on the reduced density matrices (we have already used all the symmetries available in the state), we expect this bound to be saturated. In the thermodynamic limit ($N_A, N \to \infty$ such that $N_A/N > 0$), we therefore argue that the level counting of the entire PES is identical to the number of the bulk quasihole excitations. This bound saturation can be proved exactly for the Laughlin states.[48]

It is beneficial to identify a set of rows and columns in $\mathbf{P}$ with the same rank as the full matrix. Consider the rows and columns labeled by the $(k,2)$-admissible partitions. This submatrix of $\mathbf{P}$ is denoted by $\tilde{\mathbf{P}}$ and has the same dimensions as $\mathbf{M}$. In Appendix B1, we show that $\tilde{\mathbf{P}}$ and $\mathbf{M}$ have the same rank. $\tilde{\mathbf{P}}$ will play a prominent role in the proof establishing the bulk-edge correspondence in the entanglement spectra.

Let us summarize the most relevant results presented in this section. We introduced the PES and argued that the entanglement level counting is identical to counting the number of quasihole states of the $(k,2)$-clustering model state with N_A particles in N_ϕ orbitals. This substantiates the conjecture that the PES indeed gives us information about the bulk excitations. Furthermore, we showed that the OEM block at fixed (N_A, L_z^A) is a submatrix of the PEM block at L_z^A. Consequently, the level counting of the OES at *fixed* N_A is smaller or equal to the PES counting *for all* angular momenta L_z^A. In the following section, we will derive clustering constraints that allow us to prove that the level counting of the OES and the PES are equal for a range of angular momenta L_z^A that depends on l_A and N_A.

V. CLUSTERING CONSTRAINTS

In this section, we introduce the $(k+1)$-body clustering constraints that relate the rank of the PEM and the OEM of the clustering model states and establish the bulk-edge correspondence in the entanglement spectra. The Read-Rezayi model wave functions $\psi_{(k,2)}(z_1, z_2, \ldots, z_N)$ are single Jack polynomials labeled by a root partition λ_0 [Eq. (3)] and a parameter $\alpha = -(k+1)$. They satisfy $(k,2)$ clustering: they are nonzero when a cluster of k particles is at the same point in space $z = z_1 = z_2 = \ldots z_k$, but vanish as the second power of the distance between the $(k+1)$st particle and the cluster as $z_{k+1} \to z$. The clustering property imposes a rich structure on $\psi_{(k,2)}(z_1, z_2, \ldots, z_N)$. All the partitions λ that arise in the expansion of $|\psi\rangle$ in the many-body occupation basis ($|\psi\rangle = \sum_\lambda b_\lambda |\lambda\rangle$) are dominated by λ_0. Furthermore, all the coefficients b_λ are known up to a multiplicative constant. In the Jacks, this constant is chosen so that $b_{\lambda_0} = 1$. In other words, the clustering property and the requirement to be the densest possible wave function determine $\psi_{(k,2)}(z_1, z_2, \ldots, z_N)$ uniquely up to an overall normalization constant. Here, we formulate the conditions imposed by clustering on $\psi_{(k,2)}(z_1, \ldots, z_N)$ as linear, homogeneous equations on the coefficients b_λ. These are called clustering constraints in

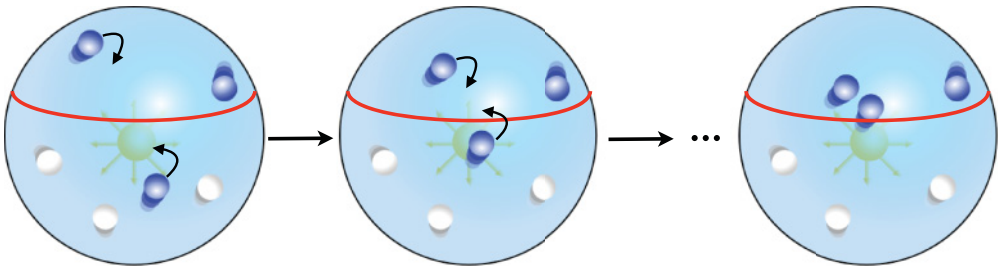

FIG. 3. (Color online) The configurations in the PES can be related to those of the OES using the clustering constraints. These constraints reveal the vanishing properties of the FQH state as particles are brought closer together. They relate the long-wavelength properties of the FQH state when two particles are far away from each other to the short-wavelength properties of the state when particles are close together, and, hence, can be used to drag particles from the PES Hilbert space into the more restrictive OES Hilbert space.

the following, and are the main tool to proof the rank equality of the PEM and OEM in Sec. VI (see Fig. 3).

A. Derivation

Let us introduce a "deletion" operator d_i for orbital i such that

$$d_i|\lambda\rangle = \begin{cases} 0, & i \notin \lambda \\ |\lambda\backslash\{i\}\rangle, & i \in \lambda \end{cases} \tag{17}$$

where $\lambda\backslash\{i\}$ is the partition with a single occurrence of the orbital i removed from it. The deletion operators commute with each other. In Appendix C, we derive the relation between these operators and the annihilation operators in the normalized single-particle basis.

We now separate the coordinates of $k+1$ particles from the rest and rewrite $\psi_{(k,2)}(z_1, z_2, \ldots, z_N)$ as

$$\psi_{(k,2)}(z_1, \ldots, z_N) = \sum_{l_1,\ldots,l_{k+1}=0}^{N_\phi} \left(\prod_{j=1}^{k+1} z_j^{l_j} \right) \langle z_{k+2}, \ldots, z_N | \prod_{j=1}^{k+1} d_{l_j} |\psi\rangle , \tag{18}$$

and form a cluster by bringing the k particles with coordinates $z_1, \ldots, z_k$ to the same position z. When $z_{k+1} = z$, the left-hand side vanishes and Eq. (18) becomes

$$0 = \sum_{l_1,\ldots,l_{k+1}=0}^{N_\phi} z^{\sum_{j=1}^{k+1} l_j} \langle z_{k+2}, \ldots, z_N | \prod_{i=1}^{k+1} d_{l_i} |\psi\rangle . \tag{19}$$

The right-hand side is a polynomial in an arbitrary complex number z and has to vanish for every power $\beta = \sum_{j=1}^{k+1} l_j$ of z to satisfy the above equation. Thus, the constraints on $|\psi\rangle$ are

$$\left(\sum_{l_1,\ldots,l_k=0}^{N_\phi} d_{\beta - \sum_{j=1}^{k} l_j} \prod_{j=1}^{k} d_{l_j} \right) |\psi\rangle = D_\beta |\psi\rangle = 0. \tag{20}$$

β is the z angular momentum of $(k+1)$ particles; it ranges from 0 to $N_\phi(k+1)$. The equation above requires any clustering wave function $|\psi\rangle$ to be simultaneously annihilated by the destruction operators $\{D_i, i = 0 \ldots N_\phi(k+1)\}$.

B. Properties

Every value of β in Eq. (20) yields, in general, a large number of linear relations between the coefficients of $|\psi\rangle$. Let S_β be the set of all partitions of N particles such that the sum of the z angular momentum of $(k+1)$ particles is β. For *every* occupation configuration of $N-(k+1)$ particles, Eq. (20) relates the coefficients of partitions $\lambda \in S_\beta$ in the expansion of $|\psi\rangle$. Examples of such relations are given in Appendix D.

The set of linear, homogeneous equations in Eq. (20) are linearly dependent. The dimension of the null space of the set is *exactly* one for the densest possible wave function, i.e., the vector of coefficients $\{b_\lambda\}$ is uniquely determined up to an overall multiplicative factor. Since the solution to Eq. (20) causes ψ to vanish when any cluster of size greater than k is formed in real space, we conclude that the set in Eq. (20) includes *all* constraints imposed on $\psi(z_1, \ldots, z_N)$ due to clustering.

Equivalently, we are describing model FQH wave functions that are the unique, highest-density zero modes of the Haldane pseudopotentials or their generalization to the $k+1$-body interaction.[39] In fact, the destruction operators above are the fundamental clustering operators from which the Haldane pseudopotentials can be obtained as the translationally invariant supersymmetric form

$$H = \sum_\beta f(\beta) D_\beta^\dagger D_\beta . \tag{21}$$

$f(\beta)$ can be derived at each k; in Appendix C, we work through the $k=1$ case.

VI. RELATING THE OES AND PES COUNTING

We now have all the ingredients necessary to relate the level counting of the PES to that of the OES for a given number of particles N_A in A and cut l_A in orbital space and prove the bulk-edge correspondence in the entanglement spectra. Let us first recap our findings so far. In Sec. IV C, we constructed the full PEM $\mathbf{P_f}$ for $(k,2)$-clustering model states and argued that the PES level counting is equal to the number of quasihole states of the same model state with N_A particles in N_ϕ orbitals. For angular momenta $L_z^A \leqslant L_{z,\min}^A + \lfloor N_A/k \rfloor$, the quasihole state counting is universal and identical to the counting of modes of the edge CFT.

For given L_z^A, we identified the submatrix $\tilde{\mathbf{P}}$ of the PEM block $\mathbf{P}$, with rows and columns labeled by $(k,2)$-admissible partitions, which has the same rank as the PEM block $\mathbf{P}$ (see Fig. 4). The block of the OEM $\mathbf{C}$ at (N_A, L_z^A) is a submatrix of

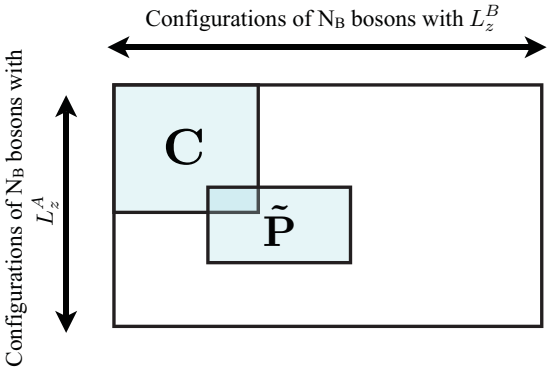

FIG. 4. (Color online) A cartoon of the various submatrices in the PEM block labeled by the angular momentum L_z^A. The block of the OEM labeled by (N_A, L_z^A) (**C** in the figure) is a submatrix of the PEM block **P** at L_z^A. $\tilde{\mathbf{P}}$ is a submatrix of **P** containing all rows and columns that are labeled by $(k,2)$-admissible partitions of N_A and N_B particles subject to total flux N_ϕ.

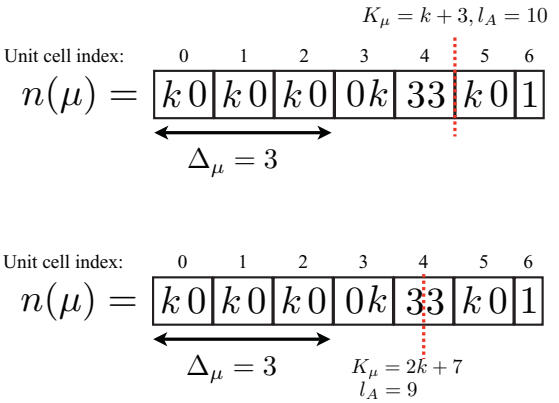

FIG. 5. (Color online) The occupation configuration of a generic partition μ with the unit cells, the number of intact unit cells Δ_μ, and the distance from cuts after $l_A = 9$ (top) and $l_A = 10$ (bottom) shown. $N_\phi = 12$ here.

the PEM block, thus, rank(**P**) $\geqslant$ rank(**C**). In order to show that the ranks are equal, we use the clustering constraints derived in the preceding section to express the row and column vectors of **P** that constitute $\tilde{\mathbf{P}}$ in terms of those that constitute the OEM block. In the following, we will refer to this as expressing the row and column vectors of $\tilde{\mathbf{P}}$ in terms of the row and column vectors of **C** even though, strictly speaking, the two matrices have different row and column dimension and can not be expressed in terms of each other. One should always think of the linear relations we derive as linear relations between rows and columns in the bigger matrix **P**, which contains both $\tilde{\mathbf{P}}$ and **C**. For finite system sizes, we show that the ranks are equal for a certain range of angular momenta, which depends on N_A and l_A [see Eq. (25)]. This proves that the PES and the OES (at fixed N_A) have the same level counting for a finite range of angular momentum. In the thermodynamic limit, this procedure establishes the equality of the level counting of the *entire* PES and OES when, roughly speaking, $N_A \approx N_{A,\mathrm{nat}}$, thus proving a significant part of the Li-Haldane conjecture.

The argument below applies equally well to row and column vectors. To keep the discussion concise, we formulate it using row vectors alone.

A. Systemizing the constraints

The biggest challenge in relating the row vectors of the PEM to those in the OEM for fixed (N_A, L_z^A) lies in identifying a set of linearly independent equations in the entire set of clustering constraints. To this end, we introduce a few quantities characterizing a partition μ. $n_m(\mu)$ below refers to the occupation number of the mth orbital in partition μ. The orbital cut is after l_A orbitals.

The unit cell: We divide the single-particle orbital space such that the jth unit cell contains the orbitals of z angular momentum $2j$ and $2j+1$, and $j \in [0, \ldots, N_\phi/2)$. As the total number of single-particle orbitals is odd for the bosonic $(k,2)$-clustering states, the orbital with angular momentum N_ϕ is its own unit cell with index $N_\phi/2$. Every orbital belongs to exactly one unit cell.

The intact unit cell: The jth unit cell of a partition μ is said to be intact if the occupation numbers of the orbitals with angular momentum $0, \ldots, 2j+1$ are identical to those in the root configuration Eq. (3), i.e., if $n_i(\mu) = n_i(\lambda_0)$ for $i = 0, \ldots, 2j+1$. Clearly, the jth unit cell can only be intact if all unit cells $0, \ldots, j-1$ are intact.

The number of intact unit cells in part A: The number of intact unit cells in part A, Δ_μ, is the number of intact unit cells to the left of the orbital cut in $n(\mu)$.

Distance from the cut: If we were to number the orbitals to the right of the cut as $1, 2, \ldots$, then the distance from the cut is defined as the sum of the indices of the occupied orbitals to the right of the orbital cut in $n(\mu)$. The distance from the cut K_μ is given by

$$K_\mu = \sum_{m=l_A}^{N_\phi} n_m(\mu)(m - l_A + 1). \tag{22}$$

$K(\mu) = 0$ for a partition μ labeling a row of the OEM; for a general partition, it represents the distance in orbital units that all the particles to the right of the cut need to traverse to cross the cut. In Fig. 5, we pick as an example a generic partition μ and identify the number of intact unit cells in A, Δ_μ, and the distance from the cut K_μ for two different orbital cuts.

Root configuration of part A: For given N_A and L_z^A, there is a unique $(k,2)$-admissible (root) configuration $n(\tilde{\mu}_0)$, with the property that $\tilde{\mu}_0$ dominates all the other partitions at angular momentum L_z^A that label rows of the PEM:

$$n(\tilde{\mu}_0) = \{\underbrace{k0\ldots k0}_{2\lfloor (N_A-1)/k \rfloor}\, x\, \underbrace{0\ldots 0}_{\ell-1} 10\ldots 0\}. \tag{23}$$

The value of x is fixed by the total particle number being N_A [$x = (N_A - 1) - k\lfloor (N_A - 1)/k \rfloor$]. $\tilde{\mu}_0$ has the maximum (total) number of intact unit cells possible, $\lfloor (N_A - 1)/k \rfloor$.

B. Method

Consider $\tilde{\mathbf{P}}$ at L_z^A and the OEM block **C** at (N_A, L_z^A) with $L_z^A = L_{z,\min}^A + \ell$. We can express all row vectors of $\tilde{\mathbf{P}}$ in terms of row vectors in the OEM block if the root configuration of

part A satisfies

$$\Delta_{\tilde{\mu}_0} \geqslant K_{\tilde{\mu}_0}. \tag{24}$$

For fixed l_A and N_A, relation (24) is fulfilled for angular momenta $L_z^A - L_{z,\min}^A = 0, \ldots, \ell_{\max}$ with

$$\ell_{\max} = \begin{cases} \Delta_{\tilde{\mu}_0} - k\bar{\Delta}_{\tilde{\mu}_0}^2 - (2\bar{\Delta}_{\tilde{\mu}_0}+1)(x+1) & \text{for } l_A \text{ even}, l_A \leqslant 2\lfloor (N_A-1)/k \rfloor, \\ \Delta_{\tilde{\mu}_0} - k\bar{\Delta}_{\tilde{\mu}_0}(\bar{\Delta}_{\tilde{\mu}_0}-1) - 2(x+1)\bar{\Delta}_{\tilde{\mu}_0} & \text{for } l_A \text{ odd}, l_A \leqslant 2\lfloor (N_A-1)/k \rfloor, \\ l_A - \Delta_{\tilde{\mu}_0} - 1 & \text{for } l_A > 2\lfloor (N_A-1)/k \rfloor, \end{cases} \tag{25}$$

where we abbreviated the difference of the total number of unit cells and those only in A by $\bar{\Delta}_{\tilde{\mu}_0} = \lfloor (N_A-1)/k \rfloor - \Delta_{\tilde{\mu}_0}$. Note that $\Delta_{\tilde{\mu}_0} = \min[\lfloor l_A/2 \rfloor, \lfloor (N_A-1)/k \rfloor]$, $\bar{\Delta}_{\tilde{\mu}_0}$, and $x = (N_A-1) - k\lfloor (N_A-1)/k \rfloor$ depend only on N_A and l_A. Thus, for all combinations (N_A, l_A), Eq. (25) gives the range of angular momenta $L_z^A = L_{z,\min}^A, \ldots, L_{z,\min}^A + \ell_{\max}$ for which all rows of the larger PEM block **P** can be expressed as linear combinations of the rows of the OEM block **C** only.

For values of $\ell \leqslant \ell_{\max}$, the proof can be broken into two steps.

(I) If $\Delta_{\tilde{\mu}_0} \geqslant K_{\tilde{\mu}_0}$, then $\Delta_{\tilde{\mu}} \geqslant K_{\tilde{\mu}}$ for all $(k,2)$-admissible partitions $\tilde{\mu} < \tilde{\mu}_0$.

(II) If $\Delta_\mu \geqslant K_\mu$ for a partition μ, then the row vector labeled by μ in **P** can be expressed as a linear combination of row vectors in the OEM **C** alone.

We prove these statements rigorously in Appendices E and F. The first step shows that the $\Delta_{\tilde{\mu}} \geqslant K_{\tilde{\mu}}$ for all partitions $\tilde{\mu}$ labeling rows of $\tilde{P}$; the second ensures that all these rows can be written as linear combinations of rows in the OEM alone.

To establish the rank equality between the PEM block **P** and the OEM block **C** with labels (N_A, L_z^A), we have to express both the rows and the columns of the PEM block in terms of those of the OEM block. An identical argument as shown above can be repeated for the column vectors. Let $\tilde{\nu}_0$ be the $(k,2)$-admissible partition that dominates all partitions of L_z^B into N_B parts. For values of ℓ such that $\Delta_{\tilde{\mu}_0} \geqslant K_{\tilde{\mu}_0}$ and $\Delta_{\tilde{\nu}_0} \geqslant K_{\tilde{\nu}_0}$, the OEM and PEM have the same counting in finite size and $\mathrm{rank}(\mathbf{P}) = \mathrm{rank}(\mathbf{C})$.

The heart of the proof lies in the use of the $(k+1)$-clustering condition (20) at the z angular momentum of the k particles in the rightmost intact unit cell in part A and one particle occupying an orbital to the right of the cut. This relates a *single* row vector belonging to the PEM block with Δ_μ and K_μ to row vectors with $\Delta_{\mu'} = \Delta_\mu - 1$ and $K_{\mu'} \leqslant K_\mu - 1$. This relation is obtained by using the clustering operator D_β with

$$\beta = 2k(\Delta_\mu - 1) + \mu_1, \tag{26}$$

where μ_1 is the angular momentum of the rightmost particle to the right of the orbital cut. The clustering constraints thus allow us to replace a row vector, the partition of which has distance K_μ with a linear combination of row vectors, the partitions of which have distances reduced by *at least* one at the cost of using a *single* intact unit cell. If $\Delta_\mu \geqslant K_\mu$ for a partition μ, then iterating this procedure provides a linear relation between the row vector labeled by partition μ and row vectors with distance zero, i.e., row vectors of the OEM block **C**.

To clarify our statements, we consider the special case of the natural spectrum $N_A = N_{A,\mathrm{nat}} = k\lfloor (l_A+1)/2 \rfloor$ for given l_A. It is straightforward to see that $l_A > 2\lfloor (N_A-1)/k \rfloor$ and $l_B > 2\lfloor (N_B-1)/k \rfloor$, so for both the rows and columns, $\ell_{\max}$ is given by the third line in Eq. (25). For the natural spectrum, the number of intact unit cells in part A is $\Delta_{\tilde{\mu}_0} = N_A/k - 1$; for part B, it is $\Delta_{\tilde{\nu}_0} = N_B/k - 1$. Consequently, we can express the rows of the PEM block in terms of rows of the OEM block for values $\ell = 0, \ldots, l_A - \lfloor (l_A+1)/2 \rfloor = \lfloor l_A/2 \rfloor$ and the columns for $\ell = 0, \ldots, \lfloor l_B/2 \rfloor$. Because we chose $l_A \leqslant l_B$, the bound from B is always larger or equal to that of A. For $\ell = 0, \ldots, N_A/k = \lfloor (l_A+1)/2 \rfloor$, we argued that the PES level counting is universal and equal to the counting of modes of the edge CFT. Thus, we find that $\mathrm{rank}(\mathbf{P}) = \mathrm{rank}(\mathbf{C})$ for $L_z^A - L_{z,\min}^A = 0, \ldots, \lfloor l_A/2 \rfloor$ and both are identical to the CFT mode counting. We can relate this range to the explicit examples given in Figs. 1 and 2, where the OES and PES level counting is indeed identical for $\ell = 0, \ldots, \lfloor 8/2 \rfloor = 4$. The range of angular momenta, for which the ranks are equal, grows linearly with system size when the ratio l_A/N_ϕ is kept constant. Small deviations from the natural number of particles do not change this picture qualitatively. In general, increasing l_A, while keeping N_A fixed, tends to raise $\ell_{\max}$, while decreasing l_A tends to lower it.

To analyze how the finite-size results carry over to the thermodynamic limit, let us fix the ratios N_A/N and l_A/N_ϕ and let $N \to \infty$. Because in that case N_A and l_A scale with N, the number of intact unit cells in A (B) in $\tilde{\mu}_0$ ($\tilde{\nu}_0$) denoted by $\Delta_{\tilde{\mu}_0}$ ($\Delta_{\tilde{\nu}_0}$) scales with N as well. There are two different scenarios: (i) If $\bar{\Delta}_{\tilde{\mu}_0}$ and/or $\bar{\Delta}_{\tilde{\nu}_0}$ grow faster than $\sqrt{N}$, then a closer look at Eq. (25) shows that $\ell_{\max} \to -\infty$ in the thermodynamic limit, i.e., our method is not applicable. (ii) If both $\bar{\Delta}_{\tilde{\mu}_0}$ and $\bar{\Delta}_{\tilde{\nu}_0}$ grow slower than $\sqrt{N}$, then $\ell_{\max}$ grows linear with system size.

As

$$\bar{\Delta}_{\tilde{\mu}_0} \sim |N_A - N_{A,\mathrm{nat}}|, \quad \bar{\Delta}_{\tilde{\nu}_0} \sim |N_B - N_{B,\mathrm{nat}}|,$$

$|N_A - N_{A,\mathrm{nat}}|$ must grow *slower* than $\sqrt{N}$. Thus, if we choose N_A (for fixed l_A/N_ϕ) such that in the thermodynamic limit $|N_A - N_{A,\mathrm{nat}}|/\sqrt{N} \to 0$ (or, equivalently, $N_A/N_{A,\mathrm{nat}} \to 1$), then Eq. (24) is satisfied for all angular momenta and the counting of the *entire* OES and PES is identical. This proves the bulk-edge correspondence in the (N_A, l_A) sectors that are most relevant in the thermodynamic limit. In particular, this includes the usual hemisphere cut ($l_A = \lfloor N_\phi/2 \rfloor$) with $N_A = k \cdot \lfloor N/(2k) \rfloor$ particles. For this choice of (N_A, l_A), the counting of the OES and the PES is identical for angular momenta range $\ell_{\max} = N/k - \lfloor N/(2k) \rfloor - 1 \approx N/(2k)$ for finite-size

systems. Thus, in the thermodynamic limit, $\ell_{\max} \to \infty$, and the counting of the OES and the PES are identical for all angular momenta.

In this section, we outlined the main steps in the proof relating the level counting of the PES and OES; the details of the proof can be found in the Appendices. For finite-size systems, Eq. (25) (and its counterpart for the column vectors) specifies the range of momenta at fixed (N_A, L_z^A) for which the level counting of the PES and OES are equal. For $N_A/N_{A,\text{nat}} \to 1$, when $N \to \infty$, this range grows linearly with system size. Hence, for this choice of (N_A, l_A), the entire level counting of the PES and OES are identical in the thermodynamic limit. For Laughlin states, one can prove that the counting of the PES is equal to the mode counting of a chiral massless boson, the CFT describing the edge.[48] Thus, the entire natural spectrum simply counts the number of edge excitations in the thermodynamic limit. We argued in Sec. IV C that the same is true for the more complicated ($k > 1$) Read-Rezayi model states; the PES counts the number of modes of the CFT describing the edge. Because of the bulk-edge correspondence in the entanglement spectra shown above, we conclude that the OES counting is equal to the number of modes of the edge CFT if we restrict N_A to be the natural number of particles in A, as specified above. This proves a significant part of the Li-Haldane conjecture.[14]

C. Illustrative examples

The proof of the full method is presented in the Appendices; here, we illustrate the more formal ideas with examples of the general method at work for the $k = 1,2$ wave functions.

1. At $k = 1$

Consider the $\nu = 1/2$ Laughlin state of $N = 7$ bosons with $N_\phi = 12$ and $L_z^{\text{tot}} = 42$. Let $l_A = 6$ and the number of particles in A be the natural number $N_A = N_{A,\text{nat}} = 3$. We consider the entanglement level counting of the OES and the PES at $L_z^A = L_{z,\min} + \ell = L_{z,\min} + 3$. We first verify that the conditions $\Delta_{\tilde{\mu}_0} \geqslant K_{\tilde{\mu}_0}$ and $\Delta_{\tilde{\nu}_0} \geqslant K_{\tilde{\nu}_0}$ are satisfied. The occupation configurations of $\tilde{\mu}_0$ and $\tilde{\nu}_0$ are

$$\begin{aligned} n(\tilde{\mu}_0) &= \{101000\,|\,0100000\}, \quad K_{\tilde{\mu}_0} = 2,\ \Delta_{\tilde{\mu}_0} = 2, \\ n(\tilde{\nu}_0) &= \{000100\,|\,0010101\}, \quad K_{\tilde{\nu}_0} = 3,\ \Delta_{\tilde{\nu}_0} = 3. \end{aligned}$$

The cut in orbital space is indicated in the occupation configurations by the "|" symbol. Hence, the method discussed in the preceding section proves the equality of the ranks of the OEM and the PEM at this L_z^A.

The occupation configurations of the (1,2)-admissible partitions labeling the rows of $\tilde{\mathbf{P}}$ are

$$\begin{aligned} n(\tilde{\mu}_0) &= \{101000\,|\,010\ldots0\}, \quad K_{\tilde{\mu}_0} = 2,\ \Delta_{\tilde{\mu}_0} = 2, \\ n(\tilde{\mu}_1) &= \{100100\,|\,100\ldots0\}, \quad K_{\tilde{\mu}_1} = 1,\ \Delta_{\tilde{\mu}_1} = 1, \\ n(\tilde{\mu}_2) &= \{010101\,|\,000\ldots0\}, \quad K_{\tilde{\mu}_2} = 0,\ \Delta_{\tilde{\mu}_2} = 0. \end{aligned} \tag{27}$$

$\tilde{\mu}_2$ labels a row that already belongs to the OEM block $\mathbf{C}$. We now relate the row labeled by the partition $\tilde{\mu}_1$ to rows of the OEM block. In $n(\tilde{\mu}_1)$, only the zeroth unit cell is intact and the particle to the right of the cut occupies the orbital with index 6. Following Eq. (26), we pick the two-body clustering constraint at $\beta = 6$ (the sum of the z angular momenta of the particle in the intact unit cell and the particle to the right of the cut) in Eq. (20):

$$[2(d_0 d_6 + d_1 d_5 + d_2 d_4) + d_3 d_3]|\psi\rangle = 0. \tag{28}$$

For every occupation-number configuration of $(N-2)$ bosons with angular momentum $(L_z^{\text{tot}} - \beta)$, Eq. (28) gives one linear relation. The appropriate occupation-number configuration for our purpose is $n([3] + \nu_j)$, as

$$d_0 d_6(|\tilde{\mu}_1 + \nu_j)) = |[3] + \nu_j\rangle\,. \tag{29}$$

The partitions ν_j of L_z^B into $N_B = 4$ parts label the columns of the PEM $\mathbf{P}$. Equation (28) then relates the row indexed by $\tilde{\mu}_1$ to row vectors indexed by the following partitions:

$$\begin{aligned} n(\mu_1) &= \{010101\,|\,000\ldots0\}, \quad K_{\mu_1} = 0,\ \Delta_{\mu_1} = 0, \\ n(\mu_2) &= \{001110\,|\,000\ldots0\}, \quad K_{\mu_2} = 0,\ \Delta_{\mu_2} = 0, \\ n(\mu_3) &= \{000300\,|\,000\ldots0\}, \quad K_{\mu_3} = 0,\ \Delta_{\mu_3} = 0\,. \end{aligned} \tag{30}$$

At every column index j, the explicit relation from Eq. (28) is

$$2(\tilde{\mathbf{P}}_{1j} + \mathbf{P}_{1j} + \mathbf{P}_{2j}) + \mathbf{P}_{3j} = 0\,, \tag{31}$$

where $\mathbf{P}_{ij}$ is the coefficient in $\mathbf{P}$ of the row labeled by μ_i and column labeled by ν_j. We have thus related a row indexed by a partition $\tilde{\mu}_1$ with $K_{\tilde{\mu}_1} = 1$ and $\Delta_{\tilde{\mu}_1} = 1$ to rows indexed by partitions μ_1, μ_2, and μ_3 with distance from the cut reduced by 1 and number of intact unit cells in A reduced by 1. These partitions label rows in the OEM in this example. A similar procedure using the additional clustering constraint at $\beta = 9$, involving the particles in the orbitals of angular momenta 2 and 7, can be used to relate the row of $\tilde{\mathbf{P}}$ indexed by the partition $\tilde{\mu}_0$ to rows in the OEM.

2. At $k = 2$

Let us now consider the Moore-Read state with $N = 18$, $N_\phi = 16$, and $L_z^{\text{tot}} = 144$ and perform an orbital cut after $l_A = 7$ orbitals. Here, we are interested in relating the rows of the PEM block to the rows of the OEM block for $N_A = 8$ at $L_z^A = L_{z,\min}^A + \ell = L_{z,\min}^A + 3$. The occupation-number configurations of $\tilde{\mu}_0$ and $\tilde{\nu}_0$ are

$$\begin{aligned} n(\tilde{\mu}_0) &= \{2020201\,|\,00100000\}, \quad K_{\tilde{\mu}_0} = 3,\ \Delta_{\tilde{\mu}_0} = 3, \\ n(\tilde{\nu}_0) &= \{0000010\,|\,01020202\}, \quad K_{\tilde{\nu}_0} = 2,\ \Delta_{\tilde{\nu}_0} = 3, \end{aligned}$$

where we indicate the orbital cut by the | symbol. Thus, $\Delta_{\tilde{\mu}_0} \geqslant K_{\tilde{\mu}_0}$ and $\Delta_{\tilde{\nu}_0} \geqslant K_{\tilde{\nu}_0}$, and we can relate all rows and columns of the PEM to those in the OEM.

The occupation configurations of the (2,2)-admissible partitions labeling the rows of $\tilde{\mathbf{P}}$ are given by

$$\begin{aligned} n(\tilde{\mu}_0) &= \{2020201\,|\,0010\ldots0\}, \quad K_{\tilde{\mu}_0} = 3,\ \Delta_{\tilde{\mu}_0} = 3, \\ n(\tilde{\mu}_1) &= \{2020200\,|\,1100\ldots0\}, \quad K_{\tilde{\mu}_1} = 3,\ \Delta_{\tilde{\mu}_1} = 3, \\ n(\tilde{\mu}_2) &= \{2020111\,|\,0100\ldots0\}, \quad K_{\tilde{\mu}_2} = 2,\ \Delta_{\tilde{\mu}_2} = 2, \\ n(\tilde{\mu}_3) &= \{2020110\,|\,2000\ldots0\}, \quad K_{\tilde{\mu}_3} = 2,\ \Delta_{\tilde{\mu}_3} = 2, \\ n(\tilde{\mu}_4) &= \{2011111\,|\,1000\ldots0\}, \quad K_{\tilde{\mu}_4} = 1,\ \Delta_{\tilde{\mu}_4} = 1\,. \end{aligned} \tag{32}$$

The trailing 0's in every occupation configuration indicate that the orbitals with $L_z = 10, \ldots, 16$ are unoccupied in the partitions labeling the rows of $\tilde{\mathbf{P}}$. $\Delta_{\tilde{\mu}_i} \geqslant K_{\tilde{\mu}_i}$ is satisfied for all $i = 0, \ldots, 4$, as required in step (i) in Sec. VI B.

We illustrate the use of the three-body clustering constraints by relating the row labeled by the partition $\tilde{\mu}_3$ to rows labeled by partitions μ_j with distance $K_{\mu_j} = 1$ from the cut. The first unit cell is the rightmost intact unit cell in A in $n(\tilde{\mu}_3)$. Consider the three-body clustering condition at β equal to the z angular momentum of the two particles in the rightmost intact unit cell and a particle to the right of the cut, i.e., at $\beta = 11 = 2 \times 2 + 7$ [see Eq. (26)]. It is beneficial to divide the clustering condition (20) into two terms:

$$3\big(D_{11}^{(1)} + D_{11}^{(2)}\big)|\psi\rangle = 0, \tag{33}$$

where

$$\begin{aligned} D_{11}^{(1)} &= d_2 d_2 d_7 + 2 d_2 d_3 d_6 + 2 d_2 d_4 d_5 + d_3 d_3 d_5 + d_3 d_4 d_4, \\ D_{11}^{(2)} &= d_0 d_0 d_{11} + 2 d_0 d_1 d_{10} + 2 d_0 d_2 d_9 + \cdots, \end{aligned} \tag{34}$$

where $D_{11}^{(2)}$ contains all terms involving angular momentum orbitals 0 and/or 1.

The clustering constraints in Eq. (33) yield a linear relation between certain coefficients in $|\psi\rangle$ for each occupation-number configuration of the remaining $N - 3$ particles. We choose the configurations $n([7,5,4,0,0] + \nu_j)$ as

$$|[7,5,4,0,0] + \nu_j\rangle = d_2 d_2 d_7 (|\tilde{\mu}_3 + \nu_j\rangle), \tag{35}$$

where the $|\nu_j\rangle$ label the column vectors of the PEM block. Note that $d_2 d_2 d_7$ is the only term in $D_{11}^{(1)}$ that contains the angular momentum 7 orbital; all other terms have highest angular momentum less than or equal to 6, and thus smaller distance to the cut. Equivalently, we can note that, as D_{11}^{1} annihilates any configuration with an occupied orbital of z angular momentum greater than 7, the first term in Eq. (33) relates the row labeled by $\tilde{\mu}_3$ only to rows labeled by partitions that are dominated by $\tilde{\mu}_3$:

$$\begin{aligned} n(\mu_1) &= \{2011111 \,|\, 1000\ldots0\}, \quad K_{\mu_1} = 1,\ \Delta_{\mu_1} = 1, \\ n(\mu_2) &= \{2010220 \,|\, 1000\ldots0\}, \quad K_{\mu_2} = 1,\ \Delta_{\mu_2} = 1, \\ n(\mu_3) &= \{2002120 \,|\, 1000\ldots0\}, \quad K_{\mu_3} = 1,\ \Delta_{\mu_3} = 1, \\ n(\mu_4) &= \{2001310 \,|\, 1000\ldots0\}, \quad K_{\mu_4} = 1,\ \Delta_{\mu_4} = 1\,. \end{aligned} \tag{36}$$

All the partitions above have one less intact unit cell and smaller distance $K_{\mu_j} = K_{\tilde{\mu}_3} - 1$ from the cut as compared to $\tilde{\mu}_3$.

The second operator in the clustering condition (33) acts on states with occupation-number configurations such as

$$\begin{aligned} &\{4000110 \mid 100010\ldots0\}, \\ &\{3100110 \mid 100100\ldots0\}, \\ &\{3010110 \mid 101000\ldots0\}, \\ &\{3001110 \mid 110000\ldots0\}, \\ &\qquad\vdots\,. \end{aligned}$$

All the above configurations have distance from the cut larger than $K_{\tilde{\mu}_3} = 2$ and *more than two particles* in angular momentum orbitals 0 and 1. Hence, they are not dominated by the root partition λ_0 and have zero weight in the model wave function (the corresponding row in the PEM is identically 0).

Thus, the clustering condition at $\beta = 11$ for the configuration of the remaining particles being $n([7,5,4,0,0] + \nu_j)$ yields a linear relation between the row labeled by $\tilde{\mu}_3$ and the rows labeled by the partitions $\mu_1, \ldots, \mu_4$:

$$\tilde{\mathbf{P}}_{3j} + 2\mathbf{P}_{1j} + 2\mathbf{P}_{2j} + \mathbf{P}_{3j} + \mathbf{P}_{4j} = 0\,, \tag{37}$$

where $\mathbf{P}_{ij}$ is the coefficient in $\mathbf{P}$ in the row labeled by μ_i and column labeled by ν_j. The rows labeled by $\mu_1, \ldots, \mu_4$ can in turn be related to rows in the OEM by using the clustering constraints at $\beta = 7$.

D. Beyond $(k,2)$-clustering states

Until now, we have restricted our discussions to the bosonic $(k,2)$-clustering states $\psi_{(k,2)}(z_1, \ldots, z_N)$. In this section, we generalize our results to other states with the property of clustering: the states obtained by multiplying $(k,2)$-clustering states with M Jastrow factors and the $(2,3)$-clustering Gaffnian state. We believe that our results hold for *all* highest-density states uniquely defined by clustering, as, for instance, the Haffnian state. For the nonunitary states, which are supposedly bulk gapless,[49,50] the map relates the counting of the OES to the number of bulk quasihole states (which is equal to the counting of the PES); however, in this case, the number of bulk quasiholes is *not* equal to the number of the edge modes, as the edge-bulk correspondence in the energy spectrum does not hold for nonunitary states.

For the $(k,2)$-clustering states, we identified a submatrix of the PEM $\tilde{\mathbf{P}}$, with the same rank as the PEM block with angular momentum label L_z^A and whose smaller dimension was the number of distinct bulk quasihole excitations. We then argued, based on the lack of other symmetries in $\tilde{\mathbf{P}}$, that its rank was equal to the smaller dimension and that the PES counted the number of bulk quasi-hole excitations at each angular momentum. To generalize this argument to other clustering states, we need to first identify the special submatrix $\tilde{\mathbf{P}}$. We can then establish the bulk-edge correspondence in their entanglement spectra by slightly modifying the method used in Sec. VI B. Extending the ideas in Sec. VI is quite straightforward: We redefine the notion of unit cell and the intact unit cell, and identify N_c, the number of linearly independent clustering constraints that involve the k particles of an intact unit cell and one particle to the right of the cut, for a fixed occupation configuration of the remaining $N - (k+1)$ particles. $N_c = 1$ for the $(k,2)$-clustering model states. Using the N_c-independent linear equations, we can relate a row labeled by a partition μ with Δ_μ intact unit cells and distance to the cut K_μ to rows labeled by partitions μ', such that $\Delta_{\mu'} = \Delta_\mu - 1$ and $K_{\mu'} \leqslant K_\mu - N_c$. Thus, in the notation of Sec. VI, when $\Delta_{\tilde{\mu}_0} \geqslant K_{\tilde{\mu}_0}/N_c$ and $\Delta_{\tilde{\nu}_0} \geqslant K_{\tilde{\nu}_0}/N_c$, the OES (at fixed N_A) and the PES have the same counting. In the thermodynamic limit, the arguments in the last paragraph in Sec. VI show that the Li-Haldane conjecture is true for these states as well when $N_A \approx N_{A,\mathrm{nat}}$.

1. (k,2)-clustering state multiplied by Jastrow factors

Let us consider the model wave function

$$\psi(z_1,\dots z_N)=\psi_{(k,2)}(z_1,\dots z_N)\prod_{i<j}(z_i-z_j)^M, \quad (38)$$

where $\psi_{(k,2)}(z_1,\dots z_N)$ is the $(k,2)$-clustering state. In Appendix B2, we show that $\tilde{\mathbf{P}}$ is labeled by row and column occupation configurations that obey the generalized Pauli principle: no more than one particle in M consecutive orbitals and no more than k particles in $Mk+2$ consecutive orbitals. The unit cell has $(Mk+2)$ orbitals and the occupation configuration of the intact unit cell is $\{1(0)^{M-1}1(0)^{M-1}\dots 1(0)^{M-1}00\}$ with $1(0)^{M-1}$ repeated k times (we could succinctly write the whole pattern as $\{[1(0)^{M-1}]^k00\}$). The exponent is the number of times the pattern in the parentheses is repeated. In Appendix G2, we show that $N_c=1$ for $M=1$. More generally, $N_c=\lfloor M/2\rfloor+1$ for $k=1$ Laughlin states, and $N_c=2\lfloor M/2\rfloor+1$ for states with $k>1$.

2. Gaffnian state

The Gaffnian state is a (2,3)-clustering state and is a single Jack polynomial

$$\psi(z_1,\dots z_N)=J^{\alpha}_{\lambda_0}(z_1,\dots z_N), \quad (39)$$

where $\alpha=-3/2$ and $n(\lambda_0)=\{200200\dots2002\}$. It is described by a nonunitary CFT, the $W_2(3,5)$ model.[51,52] It has been suggested that the fermionic Gaffnian state is the critical state between a strong-pairing phase and a Read-Rezayi phase.[53] Despite the Gaffnian being a gapless state, we can determine the counting of the PES and establish the correspondence in counting between the orbital and particle entanglement spectra. The discussion in Sec. IV C and Appendix B 1 applies to any Jack polynomial with (k,r) clustering that is a unique zero mode of a pseudopotential Hamiltonian [aside from the $(k,2)$ Jacks, only one other Jack (2,3), the Gaffnian, satisfies this constraint]. $\tilde{\mathbf{P}}$ is therefore the submatrix of the PEM labeled by (2,3)-admissible row and column occupation-number configurations for the Gaffnian state. The unit cell has three orbitals and the occupation configuration of the intact unit cell is {200}. We derive the clustering constraints in Appendix G 1 and show that $N_c=2$ for the Gaffnian.

3. Haffnian state

The Haffnian state[54] is a (2,4)-clustering state, but is not a single Jack polynomial. We can not rigorously identify $\tilde{\mathbf{P}}$ for the Haffnian state, although we expect, based on our understanding of the other model states, that $\tilde{\mathbf{P}}$ only contains the rows and columns labeled by partitions obeying the generalized Pauli principle discussed in Ref. 55. We have verified this numerically. The occupation configuration of the intact unit cell is {2000}. The clustering constraints are derived along the same lines as for the Gaffnian in Appendix G 1, giving $N_c=3$ for the Haffnian. Whenever $\Delta_{\bar{\mu}_0}\geqslant K_{\bar{\mu}_0}/3$ and $\Delta_{\bar{\nu}_0}\geqslant K_{\bar{\nu}_0}/3$, we numerically observe that the ranks of the PEM and the OEM are equal.

VII. CONCLUSIONS

In this paper, we have provided a proof that the Li and Haldane natural entanglement spectrum in the thermodynamic limit is bounded from above by the number of modes of the CFT describing the edge physics. Barring the presence of extra accidental symmetries in the system, we argue that the bound should be saturated. In addition, we showed that the two different entanglement spectra we considered, the PES probing the bulk excitations and the OES probing the edge excitations, are related. In fact, they have the same entanglement level counting for a range of angular momenta, specified by Eq. (25). The universal counting is different for each model state and provides valuable information about the topological order in the FQH state. When restricting to the natural spectrum, we have proved that, in the thermodynamic limit, the level counting of the entire OES and PES are identical. Thus, we established the bulk-edge correspondence in the entanglement spectra. The main tools in proving this are the clustering constraints, which enforce the defining clustering properties of the model states in momentum space. Our method works for both unitary and nonunitary states that are defined as unique highest-density zero modes of Haldane pseudopotential Hamiltonians. In particular, it can be applied to the entire Read-Rezayi series, as well as the Gaffnian state.

ACKNOWLEDGMENTS

We acknowledge useful discussions with F. D. M. Haldane, B. Estienne, R. Santachiara, R. Thomale, P. Bonderson, D. Arovas, X. L. Qi, and A. Ludwig. A.C., B.A.B., and M.H. want to thank Ecole Normale Superieure and Microsoft Station Q for generous hospitality. M.H. was supported by the Alexander-von-Humboldt foundation, the Royal Swedish Academy of Science, and NSF DMR Grant No. 0952428. N.R. was supported by the Agence Nationale de la Recherche under Grant No. ANR-JCJC-0003-01, and B.A.B. was supported by Princeton University Startup Funds, Alfred P. Sloan Foundation, NSF CAREER DMR Grant No. 095242, NSF China Grant No, 11050110420, MRSEC grant at Princeton University, and NSF DMR Grant No. 0819860.

APPENDIX A: A SIMPLE EXAMPLE

Let us consider the bosonic Laughlin wave function of $N=4$ particles at filling $\nu=1/2$. The number of flux quanta N_ϕ is 6 and $L_z^{\text{tot}}=12$. The wave function $|\psi\rangle$ can be expanded in the unnormalized basis as

$$\begin{aligned}|\psi\rangle &\equiv \sum_\lambda b_\lambda|\lambda\rangle\\ &= |6,4,2,0\rangle-2|6,4,1,1\rangle-2|5,5,2,0\rangle+4|5,5,1,1\rangle\\ &\quad+2|6,3,2,1\rangle-2|5,4,2,1\rangle+4|5,3,2,2\rangle+4|4,4,2,2\rangle\\ &\quad-2|6,3,3,0\rangle+2|5,4,3,0\rangle-6|4,4,4,0\rangle-4|5,3,3,1\rangle\\ &\quad-6|6,2,2,2\rangle+4|4,4,3,1\rangle-6|4,3,3,2\rangle+24|3,3,3,3\rangle.\end{aligned} \quad (A1)$$

We construct several orbital and particle entanglement matrices and use the clustering constraints to prove the bulk-boundary correspondence in the following sections.

1. Orbital cut

Let us cut the single-particle orbital space after $l_A = 3$ orbitals. Consider the blocks of the OEM at the natural number of particles in A: $N_A = N_{A,\mathrm{nat}} = 2$. From the above decomposition, the minimum possible angular momentum [Eq. (9)] for two particles in A is $L^A_{z,\mathrm{min}} = 2$. At this N_A and L^A_z, the Hilbert spaces of A and B are spanned by $|\mu_1\rangle = |2,0\rangle$, $|\mu_2\rangle = |1,1\rangle$ and $|\nu_1\rangle = |6,4\rangle$, $|\nu_2\rangle = |5,5\rangle$, respectively. The block $\mathbf{C}$ at $N_A = 2$ and $L^A_z = 2$ is then given by

$$\begin{array}{c} \\ |2,0\rangle \\ |1,1\rangle \end{array} \begin{array}{c} \begin{array}{cc} |6,4\rangle & |5,5\rangle \end{array} \\ \begin{pmatrix} 1 & -2 \\ -2 & 4 \end{pmatrix} \end{array}, \tag{A2}$$

where we have indicated the states labeling the rows and columns. $\mathbf{C}_{ij} = b_{\mu_i+\nu_j}$ (+ as defined in Sec. II) and $\mathrm{rank}(\mathbf{C}) = 1$.

The block $\mathbf{C}$ with $N_A = 2$, $L^A_z = L^A_{z,\mathrm{min}} + 1 = 3$ of rank 1 is

$$\begin{array}{c} \\ |2,1\rangle \end{array} \begin{array}{c} \begin{array}{cc} |6,3\rangle & |5,4\rangle \end{array} \\ \begin{pmatrix} 2 & -2 \end{pmatrix} \end{array}. \tag{A3}$$

The block $\mathbf{C}$ at $N_A = 2$, $L^A_z = L^A_{z,\mathrm{min}} + 2 = 4$, also of rank 1, is given by

$$\begin{array}{c} \\ |2,2\rangle \end{array} \begin{array}{c} \begin{array}{cc} |5,3\rangle & |4,4\rangle \end{array} \\ \begin{pmatrix} 4 & 4 \end{pmatrix} \end{array}. \tag{A4}$$

Figure 6(a) shows the numerically generated OES for the four-particle Laughlin state in the sphere geometry at 1/2 filling with $N_A = 2$ and $l_A = 3$. The counting of the entanglement levels in the spectrum equals the ranks of $\mathbf{C}$ at each L^A_z.

2. Particle cut

Let us construct the entanglement matrices for the particle cut with $N_A = 2$ by considering the real-space version of Eq. (A1): $\psi(z_1,\ldots,z_4) = \langle z_1,\ldots,z_4|\psi\rangle$ in the unnormalized real-space basis. Let us illustrate the particle cut using the basis state $\langle z_1,\ldots,z_4|6,4,1,1\rangle$ as an example. For simplicity, part A consists of particles at positions z_1 and z_2. We can write the unnormalized, symmetric polynomial as

$$\begin{aligned} &\langle z_1,\ldots,z_4|6,4,1,1\rangle \\ &\quad = S\left[z_1^6 z_2^4 z_3^1 z_4^1\right] \\ &\quad = S\left[z_1^6 z_2^4\right]\cdot S\left[z_3^1 z_4^1\right] + S\left[z_1^6 z_2^1\right]\cdot S\left[z_3^4 z_4^1\right] \\ &\qquad + S\left[z_1^4 z_2^1\right]\cdot S\left[z_3^6 z_4^1\right] + S\left[z_1^1 z_2^1\right]\cdot S\left[z_3^6 z_4^4\right]. \end{aligned} \tag{A5}$$

Thus, the coefficient of the PEM block $\mathbf{P}_2(2)$ in the row labeled by $|1,1\rangle$ and column labeled by $|6,4\rangle$ is given by $b_{[1,1]+[6,4]} = -2$. Doing the same procedure for every basis state occuring in $\psi(z_1,\ldots,z_4)$ allows us to determine the PEM blocks $\mathbf{P}_2(L^A_z)$ at the various allowed angular momenta L^A_z. At the smallest possible angular momentum $L^A_z = L^A_{z,\mathrm{min}} = 2$, the PEM and OEM are identical:

$$\begin{array}{c} \\ |2,0\rangle \\ |1,1\rangle \end{array} \begin{array}{c} \begin{array}{cc} |6,4\rangle & |5,5\rangle \end{array} \\ \begin{pmatrix} 1 & -2 \\ -2 & 4 \end{pmatrix} \end{array}. \tag{A6}$$

The Hilbert space of A at $L^A_z = L^A_{z,\mathrm{min}} + 1 = 3$ is spanned by the occupation number states $|3,0\rangle$ and $|2,1\rangle$. $|3,0\rangle$ was not a member of the Hilbert space of A for the orbital cut after $l_A = 3$ orbitals (discussed in the previous section) because the orbital with index 3 belonged to B. The PEM at $L^A_z = 3$ is given by

$$\begin{array}{c} \\ |3,0\rangle \\ |2,1\rangle \end{array} \begin{array}{c} \begin{array}{cc} |6,3\rangle & |5,4\rangle \end{array} \\ \begin{pmatrix} -2 & 2 \\ 2 & -2 \end{pmatrix} \end{array}. \tag{A7}$$

We see that the OEM (A3) for $N_A = 2$, $L^A_z = 2$ is indeed a submatrix of the PEM, as discussed in Sec. IV A.

As the last example, consider $L^A_z = L^A_{z,\mathrm{min}} + 2 = 4$. The row and the column dimension of the PEM is larger than that of the OEM in (A4):

$$\begin{array}{c} \\ |4,0\rangle \\ |3,1\rangle \\ |2,2\rangle \end{array} \begin{array}{c} \begin{array}{ccc} |6,2\rangle & |5,3\rangle & |4,4\rangle \end{array} \\ \begin{pmatrix} 1 & 2 & -6 \\ 2 & -4 & 4 \\ -6 & 4 & 4 \end{pmatrix} \end{array}. \tag{A8}$$

By inspection, we see that the OEM (A4) is the submatrix consisting only of the last row and the last two columns. The rank of the PEM at $L^A_z = 4$ is equal to two and greater than that of the corresponding OEM.

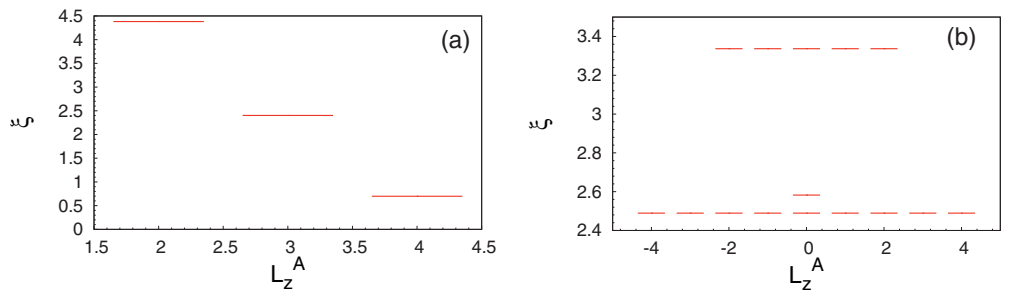

FIG. 6. (Color online) (a) Orbital entanglement spectrum of the $\nu = 1/2$ Laughlin state with $N = 4$, $N_A = 2$, and orbital cut after $l_A = 3$ orbitals. The entanglement level counting is equal to the rank of the OEM at each angular momentum. (b) Particle entanglement spectrum of the $\nu = 1/2$ Laughlin state with particle cut $N_A = 2$. The entanglement level counting at all angular momenta L^A_z is equal to the rank of the PEM. $L^A_{z,\mathrm{min}}$ defined in the text is $L^A_z = 4$ in the plots.

Figure 6(b) shows the numerically generated PES for the four-particle 1/2 Laughlin state for $N_A = 2$. The counting of the spectrum agrees with the ranks calculated above.

3. Relating the OES and PES counting

At $L_z^A = 2$, $\mathbf{C}$ [Eq. (A2)] and $\mathbf{P}$ [Eq. (A6)] are seen to be identical. There is precisely one element with a (1,2)-admissible occupation configuration in the Hilbert spaces of A and B: $|2,0\rangle$ and $|6,4\rangle$, respectively. Thus, $\tilde{\mathbf{P}} = (1)$ and the three matrices $\mathbf{P}$, $\tilde{\mathbf{P}}$, and $\mathbf{C}$ are all of rank one.

At $L_z^A = 3$, $\tilde{\mathbf{P}} = (-2)$ and is not a submatrix of $\mathbf{C}$ [Eq. (A3)]. The matrix elements $\tilde{\mathbf{P}}_{11}$ and $\mathbf{C}_{11}$ are the coefficients of $|6,3,3,0\rangle$ and $|6,3,2,1\rangle$ in the wave function $|\psi\rangle$. The two-body clustering constraints (20) at $\beta = 3$ relate these coefficients by

$$(d_3 d_0 + d_2 d_1)|\psi\rangle = 0$$
$$\Rightarrow (\tilde{\mathbf{P}}_{11} + \mathbf{C}_{11})|6,3\rangle = 0.$$

This relation between the single element in $\tilde{\mathbf{P}}$ and $\mathbf{C}$ proves that they have the same rank.

The $L_z^A = 4$ case is interesting. Here, $\tilde{\mathbf{P}}$ is

$$\begin{array}{c} \\ |4,0\rangle \\ |3,1\rangle \end{array} \begin{array}{c} \begin{array}{cc} |6,2\rangle & |5,3\rangle \end{array} \\ \begin{pmatrix} 1 & 2 \\ 2 & -4 \end{pmatrix} \end{array}.$$

$\tilde{\mathbf{P}}$ and $\mathbf{C}$ share the column index $|5,3\rangle$, but have no row index configurations in common. A single relation between the row vectors of $\tilde{\mathbf{P}}$ and the row labeled by the partition [2,2] in $\mathbf{C}$ is provided by the two-body clustering constraints at $\beta = 4$. Without another relation, we can not relate the ranks of $\mathbf{P}$ and $\mathbf{C}$ at $L_z^A = 4$. Our proof establishing the equality of ranks of the PEM and the OEM should not and is not applicable at this angular momentum, as $K_{\tilde{\mu}_0} = 2$ and $\Delta_{\tilde{\mu}_0} = 1$ with $\tilde{\mu}_0 = [4,0]$.

APPENDIX B: RANK OF $\tilde{\mathbf{P}}$

1. $(k,2)$-clustering states

The matrices $\tilde{\mathbf{P}}$ and $\mathbf{M}$ were defined in Sec. IV C as the particle entanglement matrices with label L_z^A in the $(k,2)$-admissible occupation configuration basis and the Jack basis. In Sec. IV C, we showed that the PEM and $\mathbf{M}$ have the same counting; in this appendix, we show that $\tilde{\mathbf{P}}$ and $\mathbf{M}$ have the same rank. This proves that the counting of the PEM equals the rank of $\tilde{\mathbf{P}}$.

Suppose we are able to show that $\tilde{\mathbf{P}} = \mathbf{DMD}'$, where $\mathbf{D}^{\mathbf{T}}$ and $\mathbf{D}'$ are square triangular matrices with 1's on the diagonal and, as such, they have nonzero determinant. A theorem in linear algebra states that pre- and post-multiplying a matrix by one of triangular form with nonzero determinant leaves its rank unchanged. Thus, we only need to prove that $\tilde{\mathbf{P}} = \mathbf{DMD}'$ to conclude that $\mathrm{rank}(\tilde{\mathbf{P}}) = \mathrm{rank}(\mathbf{M})$.

The row and column dimensions of $\tilde{\mathbf{P}}$ and $\mathbf{M}$ are identical because every $(k,2)$-admissible partition μ labels the Jack J_μ^α. We may use partial ordering by dominance to order the $(k,2)$-admissible row and column configurations such that, if $\tilde{\mu}_k > \tilde{\mu}_i$, then $k \leqslant i$.

Consider a particular $(k,2)$-admissible partition $\tilde{\mu}_i$ ($\tilde{\nu}_j$) labeling the ith row (jth column) of $\tilde{\mathbf{P}}$ and $\mathbf{M}$. Let the coefficient of $|\tilde{\mu}_i\rangle$ in $|J_{\tilde{\mu}_k}^\alpha\rangle$ be $\mathbf{D}_{ik}$ and the coefficient of $|\tilde{\nu}_j\rangle$ in $|J_{\tilde{\nu}_l}^\alpha\rangle$ be $\mathbf{D}'_{lj}$. The partial ordering implies that

$$\mathbf{D}_{ik} = 0 \text{ if } k > i, \tag{B1}$$
$$\mathbf{D}_{ii} = 1, \tag{B2}$$
$$\mathbf{D}'_{lj} = 0 \text{ if } l > j, \tag{B3}$$
$$\mathbf{D}'_{jj} = 1. \tag{B4}$$

In other normalizations of Jack polynomials, $\mathbf{D}_{ii}$ is not necessarily one, but is always nonzero. By the definition of a matrix with row-echelon form, $\mathbf{D}^T$ and $\mathbf{D}'$ are in row-echelon form. Recall that

$$\sum_{i,j} \mathbf{M}_{ij} \left|J_{\tilde{\mu}_i}^\alpha\right\rangle \otimes \left|J_{\tilde{\nu}_j}^\alpha\right\rangle = \sum_{i,j} \mathbf{P}_{ij} |\mu_i\rangle \otimes |\nu_j\rangle \tag{B5}$$

in every block of the full PEM. $|\mu_i\rangle$ and $|\nu_j\rangle$ are the general occupation basis states, not just the $(k,2)$-admissible configurations. $\tilde{\mathbf{P}}$ is the submatrix of $\mathbf{P}$ labeled by $(k,2)$-admissible partitions; therefore,

$$\tilde{\mathbf{P}}_{ij} = \sum_{k,l} \mathbf{M}_{kl} \langle \tilde{\mu}_i | J_{\tilde{\mu}_k}^\alpha \rangle \langle \tilde{\nu}_j | J_{\tilde{\nu}_l}^\alpha \rangle, \tag{B6}$$

$$\tilde{\mathbf{P}}_{ij} = \sum_{k,l} \mathbf{D}_{ik} \mathbf{M}_{kl} \mathbf{D}'_{lj}$$
$$\Rightarrow \tilde{\mathbf{P}} = \mathbf{DMD}', \tag{B7}$$

which proves our statement that the rank of the PEM is given by the rank of the matrix of the coefficients indexed by the $(k,2)$-admissible partitions.

2. $(k,2)$-clustering states multiplied by Jastrow factors

We consider the PEM of states that are $(k,2)$-clustering polynomials multiplied by Jastrow factors $\prod_{i<j}(z_i - z_j)^M$ [see Eq. (38)]. Here, we identify $\tilde{\mathbf{P}}$, a submatrix of the PEM with the same rank, and find that it contains only rows (columns) that are labeled by partitions $\tilde{\gamma}_i$ ($\tilde{\eta}_j$) of N_A (N_B) particles and angular momentum L_z^A (L_z^B) that obey the generalized Pauli principle: there is no more than one particle in M consecutive orbitals and no more than k particles in $Mk + 2$ consecutive orbitals. The total flux N_ϕ of the partitions $\tilde{\gamma}_i, \tilde{\eta}_j$ is equal to the total flux of the ground state $|\psi\rangle$ being cut.

Instead of expanding $|\psi\rangle$ in terms of monomials, we can choose a different basis that incorporates all the vanishing properties of the N_A (N_B) particles among themselves:

$$\langle \{z_j\} | \psi \rangle = \sum_{i,j} \mathbf{M}_{i,j} \left(J_{\tilde{\mu}_i}^\alpha \prod_{\substack{k<k' \\ k,k' \in A}} (z_k - z_{k'})^M \right) \times \left(J_{\tilde{\nu}_j}^\alpha \prod_{\substack{l,l' \\ l,l' \in B}} (z_l - z_{l'})^M \right), \tag{B8}$$

where the Jastrow factors include only particles in parts A and B, respectively. $\tilde{\mu}_i$ ($\tilde{\nu}_j$) are $(k,2)$-admissible partitions of N_A (N_B) particles with angular momentum L_z^A (L_z^B) in

$2(N-1)+MN_B+1$ (for $\tilde{\mu}_i$) and $2(N-1)+MN_A+1$ (for $\tilde{\nu}_j$) orbitals. The matrix $\mathbf{M}=(\mathbf{M}_{ij})$ has the same rank as the PEM.

Let us, for simplicity, focus on the basis states labeling the rows of $\mathbf{M}$. The Jastrow factor can be written as a $(1,M)$-clustering Jack polynomial. Hence, both the Jack and the Jastrow states obey a dominance property. They have a root configuration with coefficient 1 that dominates any other configuration in the expansion in terms of occupation-number states. This implies that also their product

$$J^{\alpha}_{\tilde{\mu}_i}\cdot\prod_{k<k'}(z_k-z_{k'})^M \tag{B9}$$

has a root configuration $\tilde{\gamma}_i$ with expansion coefficient 1, where $(\tilde{\gamma}_i)_j=(\tilde{\mu}_i)_j+M(N-j)$. Note that the $\tilde{\gamma}_i$'s are precisely the configurations that label the rows of $\tilde{\mathbf{P}}$. In addition, the partitions $\tilde{\gamma}_i$ have the same partial ordering as the μ_i, i.e., if $\tilde{\mu}_i<\tilde{\mu}_j$, then $\tilde{\gamma}_i<\tilde{\gamma}_j$. Thus, all arguments from the previous section are applicable here as well: There are row-echelon matrices $\mathbf{D}^T$ and $\mathbf{D}'$ such that $\tilde{\mathbf{P}}=\mathbf{DMD}'$, which proves that $\mathrm{rank}(\tilde{\mathbf{P}})=\mathrm{rank}(\mathbf{M})=\mathrm{rank}(\mathbf{P})$.

APPENDIX C: MODEL HAMILTONIAN EXPRESSED AS CLUSTERING OPERATORS

We rewrite the rotationally invariant, two-body Haldane pseudopotential Hamiltonian, the zero modes of which are (1,2)-clustering states, in terms of the clustering operators introduced in Sec. V. Recall that the single-particle orbitals in the lowest Landau level form the multiplet of $L=N_\phi/2$. In the $\hat{L}_z$ basis, any two-body interaction $\hat{V}$ can be expanded as

$$H=\sum_{m_i}\langle m_1,N_\phi/2;m_2,N_\phi/2|\hat{V}|m_3,N_\phi/2;m_4,N_\phi/2\rangle \times c^\dagger_{m_1}c^\dagger_{m_2}c_{m_3}c_{m_4}. \tag{C1}$$

$c^\dagger_{m_1}$ is the creation operator of a single-particle state of $L_z=m_1$, $L=N_\Phi/2$; $c^\dagger_{m_1}|0\rangle=|m_1,N_\phi/2\rangle$. We first change basis as follows:

$$|m_1,N_\phi/2;m_2,N_\phi/2\rangle=\sum_{\ell=0}^{N_\phi}|m_1+m_2,\ell\rangle \times\langle m_1+m_2,\ell|m_1,N_\phi/2;m_2,N_\phi/2\rangle,$$

where $\langle m_1+m_2,\ell|m_1,N_\phi/2;m_2,N_\phi/2\rangle$ in the right-hand side are Clebsch-Gordan coefficients. For brevity of notation, we drop the label $N_\phi/2$ in the superscript. To determine the components of the model pseudopotential in the new basis, we recall that $\hat{V}$ is rotationally invariant (commutes with $|\hat{L}^2|$ and $\hat{L}_z$) and penalizes only the relative angular momentum of 0, thus,

$$\langle n_1,\ell_1|\hat{V}|n_2,\ell_2\rangle=\delta_{n_1,n_2}\delta_{\ell_1,\ell_2}\delta_{\ell,N_\phi}.$$

The Hamiltonian in Eq. (C1) can therefore be written as

$$H=\sum_{\beta=-N_\phi}^{N_\phi}\sum_{m_1,m_3}\langle\beta,N_\phi|m_1,N_\phi/2;\beta-m_1,N_\phi/2\rangle^\star \times\langle\beta,N_\phi|m_3,N_\phi/2;\beta-m_3,N_\phi/2\rangle \times c^\dagger_{m_1}c^\dagger_{\beta-m_1}c_{m_3}c_{\beta-m_3}. \tag{C2}$$

The creation and annihilation operators above create and destroy particles in the normalized single-particle orbitals. Let us denote the normalization of the single-particle orbital with $L_z=m$ by $\mathcal{N}(m)$. To move to the unnormalized basis, we make the transformation

$$d_m=\mathcal{N}(m)c_m. \tag{C3}$$

This set of operators is identical to the deletion operators defined in Sec. V A. In spinor coordinates (u,v), the wave function of the unnormalized orbital is

$$\langle u,v|d^\dagger_m|0\rangle=u^{N_\phi/2+m}v^{N_\phi/2-m}. \tag{C4}$$

The Clebsch-Gordan coefficients appearing in Eq. (C2) have the form

$$\langle\beta,N_\phi|m_1,N_\phi/2;\beta-m_1,N_\phi/2\rangle = K\mathcal{N}(m_1)\mathcal{N}(\beta-m_1)\sqrt{(N_\phi-\beta)!(N_\phi+\beta)!}. \tag{C5}$$

K is independent of β and m_1:

$$K=\left[\left(\frac{4\pi}{N_\phi+1}\right)^2\frac{\pi^{1/4}}{\sqrt{N_\phi!}2^{N_\phi}\sqrt{(N_\phi-1/2)!}}\right]^2. \tag{C6}$$

By substituting Eqs. (C5) and (C3) in (C2), we have

$$H=\sum_{\beta=-N_\phi}^{N_\phi}\sum_{m_1,m_3}K^2(N_\phi-\beta)! \times(N_\phi+\beta)!d^\dagger_{m_1}d^\dagger_{\beta-m_1}d_{m_3}d_{\beta-m_3}. \tag{C7}$$

By comparing the equation above with the one in the text [Eq. (21)], we see that $f(\beta)=(N_\phi-\beta)!(N_\phi+\beta)!$.

APPENDIX D: TWO EXAMPLES OF CLUSTERING CONSTRAINTS

We write down the explicit relations imposed by the $(k+1)$-body clustering constraints discussed in Sec. V on the coefficients of small wave functions at $k=1,2$. Let us first consider an example at $k=1$, i.e., the 1/2 Laughlin states. The clustering constraints are two body:

$$\sum_{i=0}^{\beta}d_{\beta-i}d_i|\psi\rangle=0 \quad \text{for} \quad \beta=0,1,\ldots,L^{\mathrm{tot}}_z. \tag{D1}$$

Consider the $N=3$, $L^{\mathrm{tot}}_z=6$ wave function in the infinite plane geometry in which the number of orbitals is not restricted to $N_\phi+1=5$ as in the case of the sphere. The Hilbert space is spanned by seven partitions $\{\lambda_i,i=\ldots7\}$. Their corresponding coefficients in $|\psi\rangle$ are $\{b_i,i=1\ldots7\}$

$$|\psi\rangle=b_1|6,0,0\rangle+b_2|5,1,0\rangle+b_3|4,2,0\rangle+b_4|3,3,0\rangle +b_5|4,1,1\rangle+b_6|3,2,1\rangle+b_7|2,2,2\rangle\,.$$

The relations at $\beta=0,1$, respectively, are

$$b_1|6,0,0\rangle=0\Rightarrow b_1=0,$$
$$b_2|5,1,0\rangle=0\Rightarrow b_2=0\,.$$

Thus, the clustering constraints assign zero weight to λ_1 and λ_2, which are not dominated by the root partition $\lambda_3=[4,2,0]$ $[n(\lambda_3)=\{10101\}]$. The values of β from 2 to 6 generate a

TABLE I. Possible occupation configurations and the clustering constraints for the $N = 3$, $\nu = 1/2$ Laughlin state at $L_z^{\text{tot}} = 6$ on the infinite plane (no restriction to the number of orbitals). On the sphere, the first two configurations have zero weight and the last two orbitals are missing as $N_\phi = 4$.

Coefficient of m_μ	$n(\mu)$	Constraint
b_1	{2000001}	$\beta = 0:\ b_1 = 0$
b_2	{1100010}	$\beta = 1:\ b_2 = 0$
b_3	{1010100}	$\beta = 2:\ 2b_3 + b_5 = 0$
b_4	{1002000}	$\beta = 3:\ b_4 + b_6 = 0$
b_5	{0200100}	$\beta = 4:\ 2b_6 + 2b_3 + b_7 = 0$
b_6	{0111000}	$\beta = 5:\ b_5 + b_6 = 0$
b_7	{0030000}	$\beta = 6:\ 2b_3 + b_4 = 0$

set of five linearly dependent equations that fix four out of the five remaining coefficients. All the relations obtained are shown in Table I. The solution in terms of the coefficient of the root partition b_3 is $\{b_1,b_2,b_3,b_4,b_5,b_6,b_7\} = \{0,0,b_3, -2b_3, -2b_3,2b_3, -6b_3\}$.

The bosonic Moore-Read state is the clustering polynomial at $k = 2$. The clustering constraints involve three particles:

$$\sum_{i,j=0}^{\beta} d_{\beta-i-j} d_i d_j |\psi\rangle = 0 \quad \text{for} \quad \beta = 0,1,\ldots,L_z^{\text{tot}}. \tag{D2}$$

Consider the six-particle wave function with $L_z^{\text{tot}} = 12$. Equation (D2) for $\beta = 0$ ensures that the weight of the partitions [4,4,4,0,0,0], [5,4,3,0,0,0] ... [12,0,0,0,0,0] not dominated by [4,4,2,2,0,0] is zero in the wave function. The number of such partitions, the coefficients of which are set to zero at $\beta = 0$, is the number of partitions of 12 into at most 3 parts. Similarly, the constraints at $\beta = 1$ set the weights of the partitions [4,4,3,1,0,0], [5,4,2,1,0,0], ... [11,1,0,0,0,0] (the number of such partitions is the number of partitions of 11 into at most 3 parts) in the wave function to zero. The linear dependence of the set of constraints in Eq. (D2) is apparent in the fact that the coefficient of the partition [7,4,1,0,0,0] is set to zero by a constraint at $\beta = 0$ and one at $\beta = 1$. The constraints at $\beta = 11,12$ are also seen to give identical relations to those at $\beta = 0,1$ for this example. The configurations [5,4,3,0,0,0] ... [12,0,0,0,0,0] are only allowed in an infinite plane geometry. On the sphere, they would involve more orbitals than $N_\phi + 1 = 5$ existent ones and would not appear in the Hilbert space of the decomposition of the Moore-Read ground state. The configurations [4,4,4,0,0,0] and [4,4,3,1,0,0] appear on the sphere but, due to the same reason as on the infinite plane, i.e., that they are not squeezed from the root partition, have zero weight.

The 16 partitions dominated by the root partition [4,4,2,2,0,0] and their corresponding coefficients in ψ are shown in the second and first columns of Table II, respectively. Let us discuss the three-body clustering at $\beta = 4$ in more detail:

$$3(d_4d_0d_0 + 2d_3d_1d_0 + d_2d_2d_0 + d_2d_1d_1)|\psi\rangle = 0\,. \tag{D3}$$

TABLE II. Possible occupation configurations and the clustering constraints for the $N = 6$ MR state at $L_z^{\text{tot}} = 12$.

	$n(\mu)$	Constraint	
b_1	{20202}	$\beta = 2:$	$b_1 + b_2 = 0$
b_2	{12102}		$b_3 + b_6 = 0$
b_3	{20121}	$\beta = 3:$	$3b_3 + 6b_7 + b_9 = 0$
b_4	{20040}		$3b_4 + 6b_8 + b_{13} = 0$
b_5	{04002}		$6b_2 + b_5 = 0$
b_6	{12021}	$\beta = 4:$	$b_1 + 2b_7 + b_{10} + b_{12} = 0$
b_7	{11211}		$b_3 + 2b_8 + b_{11} + b_{14} = 0$
b_8	{11130}		$2b_6 + b_7 + b_9 = 0$
b_9	{03111}	$\beta = 5:$	$2b_2 + 2b_7 + b_9 + b_{10} = 0$
b_{10}	{02301}		$2b_7 + 2b_{11} + b_{14} + b_{15} = 0$
b_{11}	{10320}		$2b_6 + 2b_8 + b_{13} + b_{14} = 0$
b_{12}	{10401}		$2b_3 + b_6 + b_7 = 0$
b_{13}	{03030}	$\beta = 6:$	$6b_1 + 3b_2 + 6b_7 + 3b_3 + b_{12} = 0$
b_{14}	{02220}		$6b_2 + 3b_5 + 6b_9 + 3b_6 + b_{10} = 0$
b_{15}	{01410}		$6b_3 + 3b_6 + 6b_8 + 3b_4 + b_{11} = 0$
b_{16}	{00600}		$6b_7 + 3b_9 + 6b_{14} + 3b_8 + b_{15} = 0$
			$6b_{12} + 3b_{10} + 6b_{15} + 3b_{11} + b_{16} = 0$

The four terms in Eq. (D3) individually are

$$\begin{aligned}
d_4d_0d_0|\psi\rangle &= b_1|4,2,2\rangle + b_3|3,3,2\rangle,\\
d_3d_1d_0|\psi\rangle &= b_6|4,3,1\rangle + b_7|4,2,2\rangle + b_8|3,3,2\rangle,\\
d_2d_2d_0|\psi\rangle &= b_1|4,4,0\rangle + b_7|4,3,1\rangle + b_{12}|4,2,2\rangle\\
&\quad + b_{11}|3,3,2\rangle,\\
d_2d_1d_1|\psi\rangle &= b_2|4,4,0\rangle + b_9|4,3,1\rangle + b_{10}|4,2,2\rangle\\
&\quad + b_{14}|3,3,2\rangle\,.
\end{aligned} \tag{D4}$$

The right-hand side of each of the four terms above is a linear combination of different occupation configurations of three bosons with total angular momentum $L_z^{\text{tot}} - \beta = 8$. Since different occupation configuration states are orthogonal to each other, Eq. (D3) can only be satisfied if the coefficient in front of every noninteracting many-body state is zero. Thus, we obtain four constraints on the coefficients from each of the four occupation configurations in Eq. (D4):

$$\begin{aligned}
&|4,2,2\rangle : b_1 + 2b_7 + b_{12} + b_{10} = 0,\\
&|3,3,2\rangle : b_3 + 2b_8 + b_{11} + b_{14} = 0,\\
&|4,3,1\rangle : 2b_6 + b_7 + b_9 = 0,\\
&|4,4,0\rangle : b_1 + b_2 = 0.
\end{aligned} \tag{D5}$$

The last relation also arises from the clustering constraint at $\beta = 2$.

All the relations imposed by the clustering constraints at $\beta = 2,\ldots,6$ are shown in Table II. Although not obvious, in this case as in the previous, the dimension of the null space of Eq. (D2) is 1. This can be analytically proved by realizing that the Moore-Read state is the densest unique ground state of a Haldane pseudopotential Hamiltonian, which can be written in terms of the clustering operators.

APPENDIX E: PROOF OF STEP (i) IN SEC. VI B

We now prove the statement in step (i) of Sec. VI B: $K_{\tilde{\mu}_0} \leqslant \Delta_{\tilde{\mu}_0}$ implies that $K_{\tilde{\mu}} \leqslant \Delta_{\tilde{\mu}}$ for all $(k,2)$-admissible partitions

$\tilde{\mu}$ that are dominated by $\tilde{\mu}_0$. We defined $\tilde{\mu}_0$ to be the partition that dominates all other $(k,2)$-admissible partitions at given N_A, L_z^A [Eq. (23)]:

$$n(\tilde{\mu}_0) = \underbrace{k0\ldots k0}_{2\lfloor (N_A-1)/k \rfloor}\, x\, \underbrace{0\ldots 01}_{\ell} 0\ldots 0, \tag{E1}$$

where $0 \leqslant x < k$ is fixed by the total particle number being N_A. We are given that $\Delta_{\tilde{\mu}_0} \geqslant K_{\tilde{\mu}_0}$.

The main idea how to prove this statement is to reduce the distance from the cut by squeezing particles across the cut. Squeezing with the particle just left to the cut [at angular momentum $(l_A - 1)$] can not reduce the distance, but squeezing with any other particle to the left of the cut does. Let us in the following only consider squeezing operations from orbitals with index $m_1 \geqslant l_A$ and $m_2 < l_A - 1$ to orbitals with index $m_1' = m_1 - 1$ and $m_2' = m_2 + 1$. Starting from a $(k,2)$-admissible partition, there are two choices to reduce the distance to the cut by one and still retain $(k,2)$ admissibility: either one squeezes with a particle of the rightmost unit cell, which reduces the number of unit cells by one, or one squeezes with a particle that is not in an intact unit cell. The latter may retain $(k,2)$ admissibility, depending on the occupation configuration of the remaining particles, and does not change the number of intact unit cells. All $(k,2)$-admissible configurations $\tilde{\mu}' < \tilde{\mu}_0$ can be obtained from $\tilde{\mu}_0$ by such a series of squeezings. As $K_{\tilde{\mu}_0} \leqslant \Delta_{\tilde{\mu}_0}$, they obey $K_{\tilde{\mu}'} \leqslant \Delta_{\tilde{\mu}'}$. Let us make this argument more rigorous in the following paragraphs.

The case when $K_{\tilde{\mu}_0} = 0$ is trivial. All $(k,2)$-admissible partitions have distance from the cut 0 and at least 0 intact unit cells; therefore, $K_{\tilde{\mu}} \leqslant \Delta_{\tilde{\mu}}$ for all $(k,2)$-admissible partitions $\tilde{\mu}$.

In order to prove the required statement for $K_{\tilde{\mu}_0} > 0$, we consider all $(k,2)$-admissible partitions $\tilde{\mu} < \tilde{\mu}_0$ at given, but arbitrary, $K_{\tilde{\mu}} < K_{\tilde{\mu}_0}$. Let us construct the partition μ [not necessarily $(k,2)$ admissible] at the given distance $K_{\tilde{\mu}} = K_\mu > 0$ that is dominated by all the $(k,2)$-admissible partitions. This partition can always be obtained by first reducing the distance to the cut $K_{\tilde{\mu}_0} - K_{\tilde{\mu}}$ times by squeezing each time with a particle from the rightmost intact unit cell, and afterward squeezing all the particles at angular momenta $\geqslant (l_A - 1)$ to their maximally dense configuration. The latter operation does not change the distance from the cut. Assume that the orbital to the left of the cut is unoccupied, i.e., $n_{l_A-1}(\tilde{\mu}_0) = 0$. If the number of particles to the right of the cut in $\tilde{\mu}_0$, $N_r(\tilde{\mu}_0)$, is equal to one, then the occupation-number configuration of μ is given by

$$n(\mu) = \underbrace{k0\ldots k0}_{2\Delta_\mu}\underbrace{(k-1)1\ldots(k-1)1}_{2(\Delta_{\tilde{\mu}_0}-\Delta_\mu)}\underbrace{x0\ldots 0}_{l_A-2\Delta_{\tilde{\mu}_0}}|\underbrace{0\ldots 01}_{K_\mu}, \tag{E2}$$

where we denote the orbital cut by | in the occupation configuration. For $N_r(\tilde{\mu}_0) > 1$, $n(\mu)$ is

$$n(\mu) = \underbrace{k0\ldots k0}_{2\Delta_\mu}\underbrace{(k-1)1\ldots(k-1)1(k-1)0}_{2(\Delta_{\tilde{\mu}_0}-\Delta_\mu)}|X\ldots X, \tag{E3}$$

where the sequence $X\ldots X$ denotes the occupation configuration of $[N_r(\tilde{\mu}_0)+1]$ particles at distance K_μ that is maximally squeezed.

The configurations in Eqs. (E2) and (E3) are such that the particles on the left of the cut form the densest possible $(k,2)$-admissible configuration, i.e., squeezing any two particles on the left of the cut yields a configurations that is not $(k,2)$ admissible. As the particles to the right are in their most squeezed configuration, we conclude that any $(k,2)$-admissible partition with distance to the cut K_μ dominates μ.

As compared to $n(\tilde{\mu}_0)$, the z angular momentum of the particles to the left of the cut in $n(\mu)$ is increased by $\Delta_{\tilde{\mu}_0} - \Delta_\mu$, while that of the particles to the right of the cut is reduced by $K_{\tilde{\mu}_0} - K_{\tilde{\mu}}$. Since $n(\mu)$ has the same total z angular momentum as $n(\tilde{\mu}_0)$,

$$\Delta_{\tilde{\mu}_0} - \Delta_\mu = K_{\tilde{\mu}_0} - K_\mu,$$
$$\Delta_{\tilde{\mu}_0} \geqslant K_{\tilde{\mu}_0} \Rightarrow \Delta_\mu \geqslant K_\mu.$$

As every $(k,2)$-admissible partition $\tilde{\mu}$ with distance $K_{\tilde{\mu}} = K_\mu$ that dominates μ has *at least* Δ_μ intact unit cells

$$\Delta_{\tilde{\mu}} \geqslant \Delta_\mu, \quad K_{\tilde{\mu}} = K_\mu \Rightarrow \Delta_{\tilde{\mu}} \geqslant K_{\tilde{\mu}} \tag{E4}$$

at every distance from the cut.

The argument for $n_{l_A-1}(\tilde{\mu}_0) \neq 0$ is identical to the one described above. The only difference lies in the form of $n(\mu)$:

$$n(\mu) = \underbrace{k0\ldots k0}_{2\Delta_\mu}\underbrace{(k-1)1\ldots(k-1)1}_{2(\Delta_{\tilde{\mu}_0}-\Delta_\mu)}0|X\ldots X, \tag{E5}$$

where the sequence $X\ldots X$ is the maximally squeezed configuration of $x+1$ particles [for $N_r(\tilde{\mu}_0) = 1$], respectively, $k + N_r(\tilde{\mu}_0)$ [for $N_r(\tilde{\mu}_0) > 1$] at distance K_μ.

APPENDIX F: PROOF OF STEP (II) IN SEC. VI B

1. Effect of dominance on the distance from the cut

We show that dominance, i.e., $\mu > \mu'$ implies that the distance to the cut $K_\mu \geqslant K_{\mu'}$, or that squeezing can not increase the distance from the cut. The property of dominance is defined by

$$\mu > \mu' \Rightarrow \sum_{i=1}^{n} \mu_i \geqslant \sum_{i=1}^{n} \mu_i' \tag{F1}$$

for all $n \leqslant N$. Recall that $\mu_i \geqslant \mu_j$ for $i < j$, where μ_i and μ_j are the components of the partition μ. Let us denote the number of particles to the right of the cut for any partition μ by $N_r(\mu)$. The distance from the cut K_μ can then be rewritten as

$$K_\mu = \sum_{m=l_A}^{N_\phi} n_m(\mu)(m - l_A + 1)$$
$$= \sum_{i=1}^{N_r(\mu)} (\mu_i - l_A + 1). \tag{F2}$$

When comparing the total distances for two partitions μ and μ', there are three possibilities: $N_r(\mu) = N_r(\mu')$, $N_r(\mu) > N_r(\mu')$, and $N_r(\mu) < N_r(\mu')$. We will discuss them in that order:

(i) $N_r(\mu) = N_r(\mu')$:

$$\mu > \mu' \Rightarrow \sum_{i=1}^{N_r(\mu)} \mu_i \geqslant \sum_{i=1}^{N_r(\mu)} \mu'_i$$
$$\Rightarrow \underbrace{\sum_{i=1}^{N_r(\mu)} (\mu_i - l_A + 1)}_{=K_\mu} \geqslant \underbrace{\sum_{i=1}^{N_r(\mu)} (\mu'_i - l_A + 1)}_{=K_{\mu'}} . \quad \text{(F3)}$$

Thus, $K_\mu \geqslant K_{\mu'}$.

(ii) $N_r(\mu) > N_r(\mu')$:

$$\mu > \mu' \Rightarrow \sum_{i=1}^{N_r(\mu')} \mu_i \geqslant \sum_{i=1}^{N_r(\mu')} \mu'_i$$
$$\Rightarrow \sum_{i=1}^{N_r(\mu')} (\mu_i - l_A + 1) \geqslant \underbrace{\sum_{i=1}^{N_r(\mu')} (\mu'_i - l_A + 1)}_{=K_{\mu'}} . \quad \text{(F4)}$$

As $\mu_i \geqslant l_A$ for all particles to the right of the cut, $K_\mu = \sum_{i=1}^{N_r(\mu)} (\mu_i - l_A + 1) > \sum_{i=1}^{N_r(\mu')} (\mu_i - l_A + 1)$. This shows that $K_\mu > K_{\mu'}$.

(iii) $N_r(\mu) < N_r(\mu')$:

$$\mu > \mu' \Rightarrow \sum_{i=1}^{N_r(\mu')} \mu_i \geqslant \sum_{i=1}^{N_r(\mu')} \mu'_i$$
$$\Rightarrow \underbrace{\sum_{i=1}^{N_r(\mu)} (\mu_i - l_A + 1)}_{=K_\mu} + \underbrace{\sum_{i=N_r(\mu)+1}^{N_r(\mu')} (\mu_i - l_A + 1)}_{\leqslant 0}$$
$$\geqslant \sum_{i=1}^{N_r(\mu')} (\mu'_i - l_A + 1) = K_{\mu'} . \quad \text{(F5)}$$

The second term must be $\leqslant 0$, as the particles to the left of the cut have angular momentum $\mu_i < l_A$. It is strictly negative if at least one of the μ_i for $N_r(\mu) < i \leqslant N_r(\mu')$ is smaller that $(l_A - 1)$.

Thus, $K_\mu \geqslant K_{\mu'}$ for every μ' that is dominated by μ.

2. Effect of clustering constraints

We show that the $(k+1)$-body clustering constraints presented in the body of the paper [Eq. (20)] relate partitions μ with $\Delta_\mu > 0$ intact unit cells and distance $K_\mu > 0$ from the cut to partitions μ' with number of intact unit cells given by $\Delta_\mu - 1$ and distance from the cut by $K_{\mu'} < K_\mu$.

Let us consider an arbitrary partition μ with Δ_μ intact unit cells ($2\Delta_\mu$ orbitals) and distance K_μ:

$$n(\mu) = \{\underbrace{k0\ldots k0}_{2\Delta_\mu} \underbrace{x\ldots x}_{l_A - 2\Delta_\mu} | \underbrace{x\ldots x}_{\leqslant K_\mu} 0\ldots 0\} , \quad \text{(F6)}$$

where we placed the orbital cut after l_A orbitals. In order to keep the discussion general, we denote an arbitrary occupation-number configuration by the sequence $x\ldots x$. For the orbitals to the right of the cut (with angular momentum $\geqslant l_A$), two examples of such configurations with distance from the cut K_μ are

$$\{\underbrace{k0\ldots k0}_{2\Delta_\mu} \underbrace{x\ldots x}_{l_A - 2\Delta_\mu} | \underbrace{0\ldots 0}_{K_\mu - 1} 10\ldots 0\},$$
$$\{\underbrace{k0\ldots k0}_{2\Delta_\mu} \underbrace{x\ldots x}_{l_A - 2\Delta_\mu} | K_\mu\, 0\ldots 0\} . \quad \text{(F7)}$$

Let us now analyze the clustering condition that involve the k particles of the $(\Delta_\mu - 1)$th unit cell and the rightmost particle to the right of the cut in the partition μ [Eq. (F6)]. Remember that we chose to number the intact unit cells starting from 0. We choose $\beta = 2k(\Delta_\mu - 1) + \mu_1$ for the clustering operator (20) and require the remaining $N_A - (k+1)$ particles to occupy the same orbitals as in $n(\mu)$. For instance, for the configuration in the first line of (F7), we choose $\beta = 2k(\Delta_\mu - 1) + (l_A - 1 + K_\mu)$ and require the remaining $N_A - (k+1)$ particle to have the occupation configuration

$$\{\underbrace{k0\ldots k0}_{2\Delta_\mu - 2} 00 \underbrace{x\ldots x}_{l_A - 2\Delta_\mu} | 0\ldots 0\} . \quad \text{(F8)}$$

While, for the second line, we choose $\beta = 2k(\Delta_\mu - 1) + l_A$ and the occupation-number configuration of the remaining $N_A - (k+1)$ particles to be

$$\{\underbrace{k0\ldots k0}_{2\Delta_\mu - 2} 00 \underbrace{x\ldots x}_{l_A - 2\Delta_\mu} | (K_\mu - 1)\, 0\ldots 0\} . \quad \text{(F9)}$$

In particular, the occupation configurations of the remaining particles have $\Delta_\mu - 1$ intact unit cells.

The clustering condition relates μ only to partitions that are dominated by a partition μ' of the form:

$$n(\mu') = \{\underbrace{k0\ldots k0}_{2\Delta_\mu - 2}(k-1)1 \underbrace{x\ldots x}_{l_A - 2\Delta_\mu} | \tilde{x}\ldots\tilde{x}0\ldots 0\}, \quad \text{(F10)}$$

where $\tilde{x}\ldots\tilde{x}$ is used to indicate an occupation-number configuration where the rightmost particle to the right of the cut is moved to the left by one orbital. The distance from the cut is reduced by one: $K_{\mu'} = K_\mu - 1$. For our examples in Eq. (F7), the dominating partition is given by

$$n(\mu') = \{\underbrace{k0\ldots k0}_{2\Delta_\mu - 2}(k-1)1 \underbrace{x\ldots x}_{l_A - 2\Delta_\mu} | \underbrace{0\ldots 0}_{K_\mu - 2} 10\ldots 0\} \quad \text{(F11)}$$

for the configuration of the first line of Eq. (F7), and

$$n(\mu') = \{\underbrace{k0\ldots k0}_{2\Delta_\mu - 2}(k-1)1 \underbrace{x\ldots x}_{l_A - 2\Delta_\mu} | (K_\mu - 1)\, 0\ldots 0\} \quad \text{(F12)}$$

for the configuration in the second line of Eq. (F7).

Using the results from Appendix F1, we conclude that all partitions $\mu' \neq \mu$ involved in the clustering condition have $\Delta_{\mu'} = \Delta_\mu - 1$ intact unit cells and distance from the cut $K_{\mu'} \leqslant K_\mu - 1$. The $(k+1)$-body clustering condition yields one constraint on the rows labeled by all the involved partitions. Thus, we have shown that the row labeled by μ can be written as a linear combination of the rows labeled by partitions μ' with $K_{\mu'} < K_\mu$ and one less intact unit cell.

3. Relating PEM rows to OEM rows

Let us assemble the results of the previous appendices to prove the following statement: Any PEM row labeled by a partition μ with $K_\mu \leqslant \Delta_\mu$ is linearly dependent on rows labeled by partitions $\hat{\mu}_j$ with $K_{\hat{\mu}_j} = 0$. The latter are partitions that label the rows of the OEM. We prove this statement by induction, starting with a row partition μ with $K_\mu = 1$ and $\Delta_\mu \geqslant 1$. Such a row partition is necessarily of the form

$$\{\underbrace{k0\ldots k0}_{2\Delta_\mu}\underbrace{x\ldots x}_{l_A-2\Delta_\mu}|10\ldots0\}\,. \tag{F13}$$

By using the $(k,2)$-clustering constraint for $\beta = 2k(\Delta_\mu - 1) + l_A$ and fixing the occupation configuration of the remaining $N-(k+1)$ particles to be

$$\{\underbrace{k0\ldots k0}_{2\Delta_\mu-2}00\underbrace{x\ldots x}_{l_A-2\Delta_\mu}|0\ldots0\}, \tag{F14}$$

the row partition (F13) can be related to rows labeled by $\hat{\mu}_j$, which satisfy $K_{\hat{\mu}_j} = 0$. This result is independent on Δ_μ as long as $\Delta_\mu \geqslant 1$.

For the induction hypothesis, let us now assume that all row partitions λ_j with $K_{\lambda_j} \leqslant K_\lambda$ (for given $K_\lambda > 1$) and $\Delta_{\lambda_j} \geqslant K_{\lambda_j}$ can be written as linear combinations of rows labeled by partitions $\hat{\mu}_j$ with $K_{\hat{\mu}_j} = 0$.

Now consider a row partition μ with $K_\mu = K_\lambda + 1$ and $K_\mu \leqslant \Delta_\mu$. In Appendix F 2, we have shown that a clustering condition involving any of the particles to the right of the cut and the k particles of the rightmost intact unit cell (to the left of the OEM cut) relates this partition to partitions μ' with $K_{\mu'} < K_\mu$ and $\Delta_{\mu'} = \Delta_\mu - 1$. This implies that the row partition μ is a linear combination of the row partitions λ_j. Using the induction hypothesis yields that all partitions μ with distance to the cut $K_\mu \leqslant K_\lambda + 1$ fulfilling $K_\mu \leqslant \Delta_\mu$ can be written as linear combinations of rows of the OEM. This shows that any row partition μ fulfilling $K_\mu \leqslant \Delta_\mu$ can be written as a linear combination of rows labeled by partitions $\hat{\mu}_j$ that have distance to the cut $K_{\hat{\mu}_j} = 0$. These are the partitions that label the rows of the OEM.

APPENDIX G: MORE CLUSTERING CONSTRAINTS

We derive the clustering constraints of two particular states that are uniquely defined by vanishing properties distinct from $(k,2)$. It should be possible to extend the general ideas here to other model states. For $r > 3$, or for $r = 3$ and $k > 2$, the clustering constraints derived by requiring that the polynomial wave function dies with the rth power of the difference between the coordinates of $k+1$ particles do not uniquely define the wave function.[39]

1. Gaffnian state

The bosonic Gaffnian state is a $(2,3)$-clustering state.[53,56] It vanishes as the third power between the coordinate of a cluster of two particles and that of a third particle approaching the cluster:

$$\psi_{(2,3)}(z_1,z_1,z_3,\ldots,z_N) \propto (z_{1,3})^3 \quad \text{for } z_{1,3} \to 0\,, \tag{G1}$$

where we define $z_{i,j} = z_i - z_j$. Therefore,

$$\lim_{z_{1,2},z_{1,3}\to 0} (z_{1,3})^{-\alpha}\psi_{(2,3)}(z_1,z_2,z_3,\ldots,z_N) = 0 \tag{G2}$$

for $\alpha = 0$, 1, and 2. Exactly as we did in Sec. V, we separate the coordinates z_1, z_2, and z_3 from the rest and rewrite the Gaffnian wave function as

$$\psi_{(2,3)}(z_1,\ldots,z_N) = \sum_{l_1,\ldots,l_3}\left(\prod_{j=1}^{3} z_j^{l_j}\right)\langle z_4,\ldots,z_N|\prod_{j=1}^{3} d_{l_j}|\psi\rangle, \tag{G3}$$

where the d_{l_j}'s are the destruction operators defined in Sec. V. By expanding $z_3^{l_3}$ as

$$z_3^{l_3} = [z_1 - (z_{1,3})]^{l_3} = \sum_{j=0}^{l_3}\binom{l_3}{j} z_1^{l_3-j}(-z_{1,3})^j \tag{G4}$$

and inserting (G3) into Eq. (G2), we obtain the clustering constraints

$$\sum_{l_2,l_3}\binom{l_3}{\alpha} d_{\beta-l_2-l_3}d_{l_2}d_{l_3}|\psi\rangle = 0, \quad \forall\beta \geqslant \alpha \tag{G5}$$

for $\alpha = 0,1,2$. The clustering constraints at $\alpha = 0$ are identical to those we derived for the Moore-Read state in Sec. V, as a $(2,3)$-clustering state also satisfies $(2,2)$ clustering. The set of clustering constraints at each value of β are linearly dependent; in fact, for each $\beta > 2$, the number of linearly independent clustering constraints is $N_c = 2$.

2. Fermionic $(k,2)$-clustering states

The fermionic counterpart of the $(k,2)$-clustered bosonic state is

$$\psi(z_1,\ldots,z_N) = \psi_{(k,2)}(z_1,\ldots,z_N)\cdot\prod_{i<j}(z_i - z_j)\,. \tag{G6}$$

Let us start with the simplest example, the Laughlin state for $k = 1$. From the form of the wave function $\psi = \prod_{i<j}(z_i - z_j)^3$, we see that

$$\lim_{z_{1,2}\to 0} z_{1,2}^{-\alpha}\,\psi(z_1,\ldots,z_N) = 0 \quad \text{for } \alpha = 0,1,2 \tag{G7}$$

with $z_{i,j} = z_i - z_j$. Let us introduce a fermionic deletion operator d_i that destroys a fermion in angular momentum orbital i, analogous to the bosonic case Eq. (17). We can rewrite the wave function as

$$\psi(z_1,\ldots,z_N) = \textstyle\sum_{l_1,l_2} z_1^{l_1} z_2^{l_2}\langle z_3,\ldots,z_N|d_{l_1}d_{l_2}|\psi\rangle \tag{G8}$$

and expand $z_2^{l_2}$ as

$$z_2^{l_2} = (z_1 - z_{1,2})^{l_2} = \sum_{j=0}^{l_2}\binom{l_2}{j} z_1^{l_2-j}(-z_{1,2})^j\,. \tag{G9}$$

By inserting this expression of ψ into Eq. (G6) and taking the limit $z_{1,2} \to 0$, the only nonvanishing contribution is for

$j = \alpha (= 0,1,2)$ (all others vanish trivially) and we arrive at the clustering constraints

$$0 = \sum_{l_1,l_2} \binom{l_2}{\alpha} d_{l_1} d_{l_2} |\psi\rangle. \tag{G10}$$

The condition at $\alpha = 0$ is identically zero due to the anticommutation relations of the fermionic operators.

For $\alpha = 1$, we find, using $\beta = l_1 + l_2$,

$$0 = \sum_{l=0}^{\beta} l d_{\beta - l} d_l |\psi\rangle \quad \text{for } \beta \geqslant 1. \tag{G11}$$

When applying the above conditions, one must account for the anticommutation of the fermionic deletion operators d_l. Choosing $\alpha = 2$ yields clustering constraints that are identical to those at $\alpha = 1$, up to an overall multiplicative constant. Thus, for the fermionic model state at $\nu = 1/3$, we find only one clustering condition [Eq. (G11)] as in the bosonic case.

For $k > 1$, a very similar picture emerges. The two-body clustering constraints that originate from requiring

$$\lim_{z_{1,2} \to 0} \psi(z_1, \ldots, z_N) \equiv 0 \tag{G12}$$

are equivalent to Pauli exclusion statistics. In order to find the relevant $(k+1)$-particle clustering condition, we divide the wave function by a full Jastrow factor of the particles $z_1, \ldots, z_{k+1}$:

$$0 \equiv \lim_{z_{1,2},\ldots,z_{1,k+1} \to 0} \left(\prod_{i<j}^{k+1} z_{i,j}^{-1} \right) \psi(z_1, \ldots, z_N). \tag{G13}$$

Following the same steps as in the preceding section, we find the clustering constraints

$$0 = \sum_{l_1,\ldots,l_{k+1}} \prod_{j=1}^{k+1} \binom{l_j}{j} d_{l_j} |\psi\rangle \tag{G14}$$

with $l_1 + l_2 + \ldots l_{k+1} = \beta$.

In principle, one can also analyze variants of Eq. (G13), where not a full Jastrow factor is divided out, and derive clustering constraints from them. However, the resulting conditions are identically zero due to the anticommuting operators. The only nontrivial relation is the one given in Eq. (G14).

In general, when multiplying the $(k,2)$-clustering model state with M Jastrow factors ($M > 1$), we find $\lfloor M/2 \rfloor$ two-body clustering constraints and (for $k > 1$) $\lfloor M/2 \rfloor$ three-body clustering constraints, in addition to the original $(k+1)$-body clustering constraint from the model state. Thus, the total number N_c of clustering constraints is $N_c = 2\lfloor M/2 \rfloor + 1$.

[1] S. R. White, Phys. Rev. Lett. **69**, 2863 (1992).
[2] U. Schollwöck, Rev. Mod. Phys. **77**, 259 (2005).
[3] N. Shibata and D. Yoshioka, Phys. Rev. Lett. **86**, 5755 (2001).
[4] A. E. Feiguin, E. Rezayi, C. Nayak, and S. Das Sarma, Phys. Rev. Lett. **100**, 166803 (2008).
[5] G. Vidal, Phys. Rev. Lett. **99**, 220405 (2007).
[6] F. Verstraete and J. I. Cirac, e-print arXiv:cond-mat/0407066.
[7] M. Levin and X.-G. Wen, Phys. Rev. Lett. **96**, 110405 (2006).
[8] A. Kitaev and J. Preskill, Phys. Rev. Lett. **96**, 110404 (2006).
[9] P. Calabrese and J. Cardy, J. Stat. Mech. (2004) P06002.
[10] J.-M. Stéphan, S. Furukawa, G. Misguich, and V. Pasquier, Phys. Rev. B **80**, 184421 (2009).
[11] S. Dong, E. Fradkin, R. G. Leigh, and S. Nowling, J. High Energy Phys. 05 (2008) 016.
[12] M. Haque, O. Zozulya, and K. Schoutens, Phys. Rev. Lett. **98**, 060401 (2007).
[13] A. M. Lauchli, E. J. Bergholtz, and M. Haque, New. J. Phys. **12**, 075004 (2010).
[14] H. Li and F. D. M. Haldane, Phys. Rev. Lett. **101**, 010504 (2008).
[15] R. Thomale, A. Sterdyniak, N. Regnault, and B. A. Bernevig, Phys. Rev. Lett. **104**, 180502 (2010).
[16] M. Hermanns, A. Chandran, N. Regnault, and B. Bernevig, Phys. Rev. B **84**, 121309(R) (2011).
[17] A. Sterdyniak, N. Regnault, and B. Bernevig, Phys. Rev. Lett. **106**, 100405 (2011).
[18] E. Prodan, T. L. Hughes, and B. A. Bernevig, Phys. Rev. Lett. **105**, 115501 (2010).
[19] L. Fidkowski, T. Jackson, and I. Klich, e-print arXiv:1101.0320.
[20] T. Hughes, E. Prodan, and B. Bernevig, Phys. Rev. B **83**, 245132 (2011).
[21] A. Turner, Y. Zhang, R. Mong, and A. Vishwanath, e-print arXiv:1010.4335.
[22] H. Yao and X.-L. Qi, Phys. Rev. Lett. **105**, 080501 (2010).
[23] M. Fagotti, P. Calabrese, and J. Moore, J. Stat. Mech. (2010) P09012.
[24] F. Franchini, A. R. Its, V. E. Korepin, and L. A. Takhtajan, Quantum Inf. Process. **10**, 325 (2011).
[25] A. M. Turner, F. Pollmann, and E. Berg, Phys. Rev. B **83**, 075102 (2011).
[26] F. Pollmann and J. E. Moore, New J. Phys. **12**, 025006 (2010).
[27] F. Pollmann, A. M. Turner, E. Berg, and M. Oshikawa, Phys. Rev. B **81**, 064439 (2010).
[28] D. Poilblanc, Phys. Rev. Lett. **105**, 077202 (2010).
[29] R. Thomale, D. P. Arovas, and B. A. Bernevig, Phys. Rev. Lett. **105**, 116805 (2010).
[30] P. Calabrese and A. Lefevre, Phys. Rev. A **78**, 032329 (2008).
[31] A. M. Läuchli, E. J. Bergholtz, J. Suorsa, and M. Haque, Phys. Rev. Lett. **104**, 156404 (2010).
[32] O. S. Zozulya, M. Haque, and N. Regnault, Phys. Rev. B **79**, 045409 (2009).
[33] Z. Papic, B. A. Bernevig, and N. Regnault, Phys. Rev. Lett. **106**, 056801 (2011).
[34] Z. Liu, H.-L. Guo, V. Vedral, and H. Fan, Phys. Rev. A **83**, 013620 (2011).
[35] J. Schliemann, Phys. Rev. B **83**, 115322 (2011).
[36] L. Fidkowski, Phys. Rev. Lett. **104**, 130502 (2010).
[37] A. M. Turner, Y. Zhang, and A. Vishwanath, Phys. Rev. B **82**, 241102 (2010).
[38] I. Peschel, J. Phys. A: Math. Gen. **36**, L205 (2003).

[39]S. H. Simon, E. H. Rezayi, and N. R. Cooper, Phys. Rev. B **75**, 195306 (2007).
[40]F. D. M. Haldane, Phys. Rev. Lett. **51**, 605 (1983).
[41]F. D. M. Haldane, Phys. Rev. Lett. **67**, 937 (1991).
[42]B. A. Bernevig and F. D. M. Haldane, Phys. Rev. Lett. **100**, 246802 (2008).
[43]R. Stanley, Adv. Math. **77**, 76 (1989).
[44]X.-G. Wen, Adv. Phys. **44**, 405 (1995).
[45]B. A. Bernevig and F. D. M. Haldane, Phys. Rev. B **77**, 184502 (2008).
[46]V. Gurarie and E. Rezayi, Phys. Rev. B **61**, 5473 (2000).
[47]N. Read and E. Rezayi, Phys. Rev. B **59**, 8084 (1999).
[48]B. Estienne (private communication).
[49]N. Read, Phys. Rev. B **79**, 045308 (2009).
[50]P. Bonderson, V. Gurarie, and C. Nayak, Phys. Rev. B **83**, 075303 (2011).
[51]B. Estienne and R. Santachiara, J. Phys. A: Math. Gen. **42**, 445209 (2009).
[52]B. Bernevig, V. Gurarie, and S. Simon, J. Phys. A: Math. Gen. **42**, 245206 (2009).
[53]S. H. Simon, E. H. Rezayi, N. R. Cooper, and I. Berdnikov, Phys. Rev. B **75**, 075317 (2007).
[54]D. Green, Ph.D. thesis, Yale University, 2001.
[55]M. Hermanns, N. Regnault, B. A. Bernevig, and E. Ardonne, Phys. Rev. B **83**, 241302 (2011).
[56]B. A. Bernevig and F. D. M. Haldane, Phys. Rev. Lett. **101**, 246806 (2008).